Ultrasonic Air Leak Detection: An Investigation to Improve Accuracy of Leak Rate Estimation

A thesis
submitted in fulfillment
of the requirements for the degree
of
Masters of Engineering
at
The University of Waikato
by

Hamish Roger Wolstencroft

THE UNIVERSITY OF
WAIKATO
Te Whare Wānanga o Waikato

2008

Abstract

A compressed air test rig was designed to develop new procedures and improve the reliability of results that are obtained when conducting a leak survey using an Ultrasonic leak detector such as the UE Systems Ultraprobe.

A test rig was designed that allowed the pressure of air in a compressed air system to be controlled by a regulator. This allowed experiments to be conducted that were able to recreate leak situations in a controlled environment. The pressure of the air through the test rig was measured both at the supply end and at the proximity of the leak site, while the volume flow rate was measured at the supply end of the rig.

A number of leak geometries were examined, with compressed air being passed through open ended tubing and also discs with different leak geometries, some round holes and some rectangular. Initial studies were also carried out on flange leaks and pinpricks and slits in lengths of tubing. These were omitted from the study at this stage to allow further experimentation to be conducted in both areas.

The experimentation was carried out using an Ultraprobe 9000 leak detector which was positioned at a set distance from the leak at a series of angles to the flow. The ultrasound level was measured at each point and compared with the pressure and volume flow rate of the air in the system.

The results showed that the ideal angle to ensure the maximum level of ultrasound is at 30° to the axis of the leak. While the optimum distance for ensuring a consistent level of ultrasound is 150mm from the leak.

The length of any air lines branching from the main distribution network is shown to be an important factor when quantifying the volumetric flow rate of air from an open

ended tube or tubing with a significant orifice in it. The pressure drop in a 1m length of tubing was shown to be approximately 50%, and if you consider that often the flow rate being used has been obtained using the outside diameter of the tubing rather than the inside diameter this can become a considerable over estimation of leak rate.

The geometry of a regular shaped orifice, such as a round, or rectangular hole was shown to have little to no effect on the flow rate through it for a constant area. However a coefficient of discharge to account for imperfections in the flow was developed for round and rectangular geometries, these were 0.74 for a round hole and 0.79 for a rectangular hole. These correction factors in tandem with the length effect factor for tubing and the improvements to the measurement procedure, allow a higher degree of accuracy to be obtained when conducting a leak survey.

Acknowledgments

This year has been an incredible journey for me. A little over eighteen months ago the very idea that I would be completing my Masters and embarking on a new life in New Zealand would have been inconceivable to me.

Firstly I must thank James Neale and Michael Walmsley for their supervision and hours of patience and understanding as I have tried to drag the knowledge I acquired many years ago back to the forefront of my brain. Their assistance with my Thesis has been invaluable. Without their help I would not have got this far.

I must next thank Chris Burrell, formerly of The Energy Research Group, without his timely intervention when I was on holiday in New Zealand this opportunity would never have arisen.

Peter Kamp who has given me the opportunity to further extend my knowledge, by allowing me the opportunity to continue with The Energy Research group now that my Thesis is complete.

There are many others who I would also like to thank for their help, Paul Ewart for his technical support in the lab, the workshop staff, Brian and Chris for their help getting items made and everyone else who helped me on my way.

The other members of the Energy Research group that have assisted me, Lance Wong, Martin Atkins, Jonas Hoffman-Vocke, SongXin Zhao, Andrew Morrison and Ron Smail.

My Mother, Alison who encouraged me to do this even though it was on the far side of the world. Unfortunately my father, Peter is not here to see it, but hopefully I've made him proud.

My brother and sister, Colin and Sheena who have also been extremely supportive, and who have both also been amazingly successful in their chosen careers.

Finally Fiona, my beautiful girlfriend who has not only moved across the world to be with me, but has also not seen me for several weeks, apart from at meal times. Thank you for being so supportive, I know how difficult it's been for you too.

1 Introduction

1.1 Project Rationale

With rapidly rising fuel costs and the likely introduction of environmental emission taxes, it is crucial that businesses reduce their energy usage. In an industrial plant the motors that power the air compressors are typically the plants single largest users of electricity and a properly managed compressed air system can save energy, reduce maintenance, decrease downtime, increase production throughput, and improve product quality.

One of the most important facets of a compressed air management program is leak detection. This can be done by charging up the system and shutting off all valves and machinery that use the compressed air and then over a given period see what the total pressure drop in the system is. However this is time consuming and costly and can only be done when there is scheduled plant downtime.

The simplest and least intrusive method of implementing a leak detection program is to use an ultrasonic leak detector. Using an ultrasonic device it is possible to detect air leaks above the background noise of a plant room. As it has a short wavelength ultrasound is much more directional than audible sound, this combined with the difference in frequencies make it easy to differentiate from audible sound and therefore to locate.

One example of an ultrasonic leak detector is the UE Systems Ultraprobe. This is a simple to use device that combines both an audio and visual indication of ultrasound. The user wears a set of headphones while carrying out an inspection, these heterodyne the signal allowing it to be audible to the human ear. The level of ultrasound will be displayed on the device as a dB reading allowing the signal to be quantified. While

having an audio signal is useful, the display is what makes this more than just a detector.

Ultrasonic leak detectors are used by industry as a detection device or as part of a leak management program. When used as a leak detector, an inspector will locate leaks in the plant and where necessary organise to have any leaks fixed. When used as part of a leak management program, a more structured approach to leak detection is taken, where regular inspections of the compressed air system are carried out. Leaks are tagged and categorised with the date, location and the level of ultrasound measured at the leak. The urgency of any repair will be included as part of any management program, this may include factors such as ease of access, cost of downtime, cost of parts, or impact on product quality. These factors play an important role in the decision making process as any one of them can alter the justification for carrying out a repair. Only an impact on product quality would ensure repair of a leak without question.

The main advantage of having a leak management program in place using ultrasonic leak detection, rather than the more basic principle of detect and fix, is that a regular management program can identify repetitive leaks, and, by quantifying the loss rate from a series of leaks can ensure that the compressed air system is optimised, ensuring that when problems occur the true source is identified. This leads to greater confidence when making investment decisions. One current tool that makes quantification of leaks possible is a chart that comes with the UE Systems Ultraprobe 9000/10000.

The UE Systems devices are supplied with a simple chart, called a “Guess-timator” Leak Chart that allows an ultrasound level to be cross-referenced with a system pressure to approximate the leak rate. They are frequently used by untrained inspectors to carry out air leak surveys and air audits prior to advising industry on significant investment decisions. While the current chart is a useful aid to get an approximate level of air loss, it is very basic and UE Systems advise users to include a fifty percent “discount factor” when using the chart.

1.2 Aim and Scope

As is shown in the project rationale, leak detection and quantification has come a long way in recent years, mainly driven by a need for industry to become more efficient to drive down costs in the face of rising fuel prices.

The aim of this thesis is to take the concept of the UE Systems “Guess-timator” Leak Chart and develop a more robust “Leak Characterisation” Chart, and associated procedures to accompany it, which will allow the user to quantify a leak rate for a given dB reading more accurately.

The scope of this study will be concentrate on three leak types, an open ended line, a hole, or a slot in a distribution network.

To accomplish the main goal of designing a “Leak Characterisation” Chart, three intermediate stages are to be undertaken:

1) A test rig is to be designed that will allow the different leaks to be tested under the same conditions and with good repeatability.
2) The effect of the different factors on the ultrasonic sound level will be isolated and assessed to enable categorisation of the leak types with respect to those factors.
3) The new “Leak Characterisation” chart will be developed using the results collected from (2).

1.3 Thesis Structure

To address the research questions given in 1.2 this thesis is broken into four sections. The first gives the rationale for the thesis its aims and goals and the background to the research area. The second section includes, the design of the test rig, the test pieces,

and, the experimental procedures that were used to achieve the goals of the first section. The third section contains the experimental results that form the basis for the fourth section, which covers the conclusions that were drawn from the results and their implementation into a new leak characterisation chart and leak survey procedures.

2 Compressed Air Systems

2.1 History

Compressed Air has been used for thousands of years. From its origins of people blowing on cinders to light a fire and the birth of metallurgy where the wind and then blowpipes were used to develop higher temperatures. Then came the first mechanical compressor, the hand bellows, followed by foot and water wheel driven bellows. As blast furnaces developed so did the need for air compression. In 1762, John Smeaton the first professional engineer developed a water wheel driven blowing cylinder while in 1776 inventor John Wilkinson introduced an efficient blasting machine which was an early prototype for all mechanical compressors. Until the late 18th Century air compression was used mostly for mining and fabrication of metals, supplying the air for combustion and ventilation, and from the early 19th Century the idea of using air compression for energy transmission became popular as metal manufacturing plants grew and the limited power of steam became apparent. As the 19th century progressed, uses of compressed air for energy transmission became more advanced until Austrian Engineer Viktor Popp installed a 1500kW compressor plant in 1888. This was the beginning of the compressed air plant as we know it today, where it is used for pneumatic tools, control, monitoring and regulation. (ecompressedair)

2.2 Compressed Air Systems Today

Compressed air is now used widely throughout industry and is often considered the “fourth utility”. Almost every industrial plant, from a small machine shop to an immense pulp and paper mill has a compressed air system, and in many cases, it is so vital that the facility cannot operate without it. Industrial air compressor systems can vary in size from a small unit of 5 horsepower (hp) to huge systems with more than 50,000 hp and in many facilities, they use more electricity than any other type of

equipment. Inefficiencies in compressed air systems can therefore be significant. Energy savings from system improvements can range from 20 to 50 percent or more of electricity consumption. For many facilities this is equivalent to thousands, or even hundreds of thousands of dollars of potential annual savings, depending on use. (Compressed Air Sourcebook)

2.3 Layout of Compressed Air System

A Compressed Air Plant layout is shown in Figure 2.1 with the typical components identified. Leaks will commonly occur at the following points in the system:

Couplings, hoses, tubes, and fittings.

Pressure regulators.

Open condensate traps and shut-off valves.

Pipe joints, disconnects, and thread sealants

Out of use equipment still connected to the system.

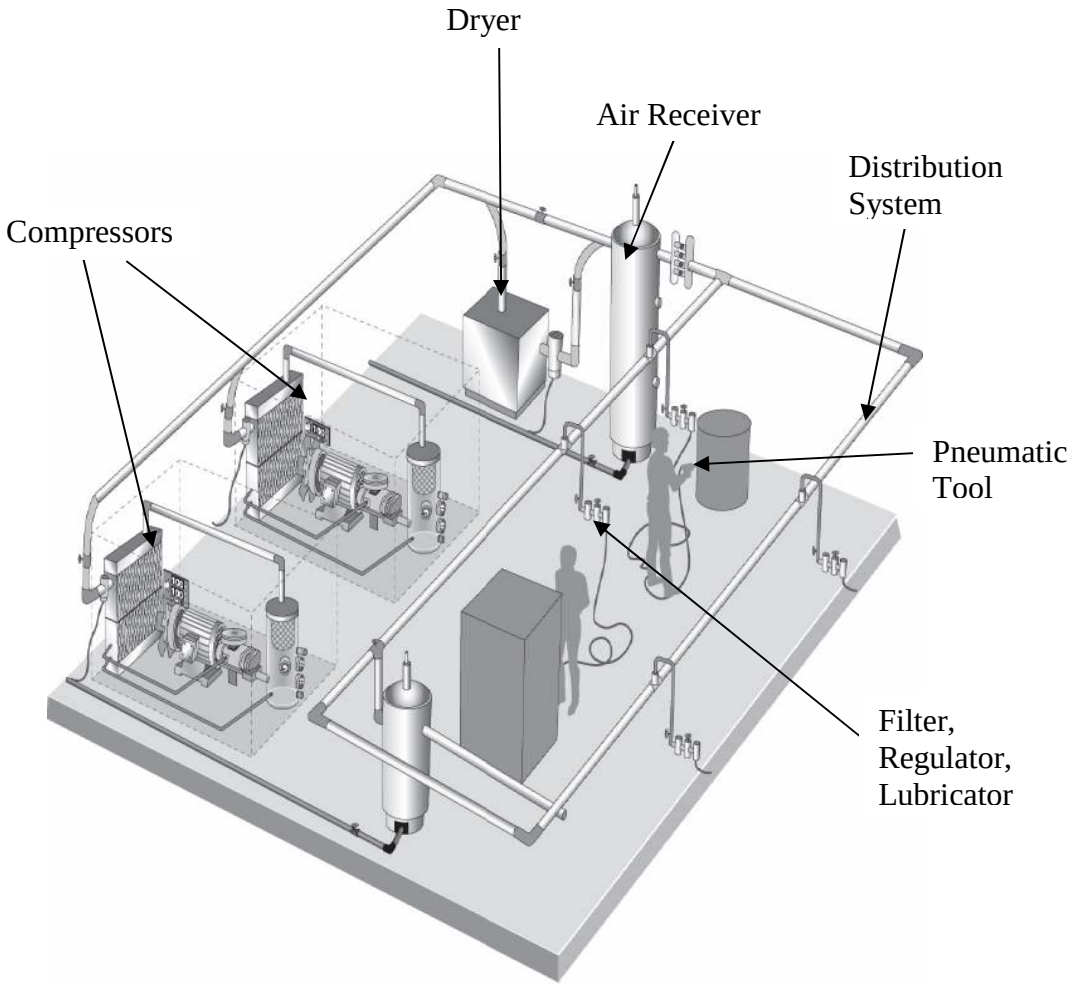

Figure 2.1, Layout of a Compressed Air System

2.4 Air Leak Detection in a Compressed Air System

Air leak detection has come a long way in the last few years, from the days of someone going round a plant with a soapy rag, to today, where ultrasound is the easiest and most reliable method of detecting leaks. Ultrasound leak detection in its most basic form involves someone going round an industrial plant, detecting leaks and fixing them, to the company who have a basic leak management program where they locate, tag and record leaks to allow a more structured approach to fixing the leaks and finally the approach that this thesis is aimed to improve.

That is the full leak management program, that identifies and tags the location of a leak, quantifies it on the basis of ultrasound level in conjunction with a “Guess-timator“ chart, (when using the UE Systems Ultraprobe), notes the accessibility of the leak, the time it will take to fix, the urgency and the date when it was identified. All this information can be loaded onto a PDA and a report printed, to ensure that an up to date record is available at all times.

The aim of this thesis is to provide additional information that can either be used as a manual set of correction factors to allow more accurate quantification of leaks, or additional data that can be included in PDA software to improve its functionality and accuracy.

The following chapter discusses the factors that affect the level of ultrasound at a leak site and is the basis for the areas of investigation of the thesis.

3 Airborne Ultrasound Leak Detection Theory

3.1 Overview

Air leaks cost industry millions of dollars every year in unnecessary compressed air production, with leaks sometimes wasting 20-30% of a compressor's output (Compressed Air Sourcebook). Detecting air leaks and deciding whether or not to fix them depends on a number of variables, for example, the cost of repair versus the cost of shutting down the plant, safety and the impact on related objects or products (e.g. product quality).

There are several factors that make a leak detectable using airborne ultrasound. Of these, the one factor that must be present is turbulence as it is this that generates the ultrasound. Orifice shape, pressure differential and atmospheric conditions will affect the level of turbulence, while competing ultrasounds, distance from the leak and accessibility to the leak are external factors that may affect the level of ultrasound measured by an airborne ultrasound leak detector. These factors each impact on the level of measured ultrasound to varying degrees.

Each factor was evaluated to assess their relationship with, or, impact on the level of measured ultrasound before a decision was taken to include them in this study.

3.2 Leak Factor Evaluation

Competing ultrasounds may affect the dB level measured by an ultrasonic leak detector but ultimately can be minimised by using one of several shielding or barrier techniques such as keeping your body between a leak and competing ultrasound, using a gloved hand to protect the tip of the probe from a competing ultrasound, or,

placing a clipboard or similar barrier between a leak and a competing ultrasound (UE Systems – Airborne Ultrasound Level 1 Handbook). As this factor is relatively easy to control by an inspector it has been excluded from this study.

As atmospheric conditions in most circumstances will have a minimal impact on the dB level measured with the exception being at altitude where the density of air is lower, this factor has been excluded from this study.

Accessibility to the leak can be a major factor in ultrasound measurement as an inability to get close to a leak impacts on the ability of an inspector to obtain an accurate estimate of the dB level. For any leak characterisation process to be accurate, the distance from the leak, and the directionality of ultrasound must be clearly understood by the inspector to ensure appropriate assessments and adjustments are made.

Due to the relatively high attenuation levels of ultrasound, the distance from the leak is an important factor in air leak detection. Ultrasonic air leak characterization relies on charts that relate a decibel reading with a volume flow rate at a given pressure and a set distance. As an approximation, the inverse distance law that gives a reduction of 6dB for every doubling of distance for audible sound is used. This study will investigate the validity of using this approximation in the ultrasonic sound range and include the findings as part of an overall air leak management plan.

When leak measurement is being conducted it is turbulence that creates the ultrasound measured by an ultrasonic leak detector, however turbulence is the product of two of the other factors rather than one in its own right. These factors are pressure differential and orifice shape. Turbulence will be discussed as part of this study to enable the reader to gain an understanding of ultrasound generation rather than as part of the experimental process.

There is a pressure differential present for all leaks, whether they are pressure leaks or vacuum leaks. It is this pressure differential that creates the turbulence at the leak site

as each side of the leak tries to equalize with the other. At present it is presumed that for any given leak, the higher the pressure differential is, the greater the turbulence and the greater the dB level. Although the pressure differential is not a variable that can be controlled by an inspector, the effect of air line diameter and length on flow rate from a given leak at a variety of line pressures will be investigated as part of this study.

The orifice shape, including the size, of any leak will have a significant effect on the level of ultrasound generated, whether it has a smooth edge or a rough edge, a round or a square cross section, if it is at a flange or fitting, or, is a small pinprick or a gaping hole, all these variables will affect the level of ultrasound being generated by the leak. This factor plays a significant role in the level of ultrasound being measured at leak sites and will therefore be included in the scope of this study

Although all the above factors may affect the level of ultrasound being measured, the two factors that are thought to have the greatest impact on the leak rate of any leak are pressure differential and orifice shape. They are the two factors that actively affect the level of turbulence from the leak and therefore the level of ultrasound generated. They will form the core of this study. Additional studies will be carried out regarding the effect of distance and directionality from the leak, of the ultrasound signal radiating from the leak.

3.3 Leak Factor Areas of Investigation

This study will investigate the following factors:

1. Orifice shape
2. Pressure differential
3. Distance from the Leak
4. Directionality

3.3.1 Orifice Shape

In any leak survey it is important to identify the location and type of leak so as to enable a decision to be made on the urgency and economics of any leak repair and also to provide details of any materials that may be required to implement a repair. This is an ideal opportunity for the shape and size of a leak to be categorized. The size and shape of a leak can give vital information to the inspector that can be included in a leak report. The testing of orifice shape in this study will include the following comparisons:

a. Round holes of various diameters.
b. Rectangular slots of various cross sectional area.
c. Rectangular slots of varying aspect ratio but constant cross sectional area.
d. Round holes against rectangular slots of constant cross sectional area.
e. Open ended tubing of various diameters.
f. Coefficient of Discharge for all geometries.

This section of the study will look for similarities and differences between leak types and sizes to allow leak geometries to be categorized into leak types with similar flow rates and ultrasonic sound level.

3.3.2 Pressure Differential

When conducting leak surveys it is common practice to obtain the ultrasonic sound level with the scanner and evaluate the leak rate on the basis of system pressure. This method takes no account of pressure drop that may occur in the system, which may lead to vastly overstated estimations of leak rate. In this study compressed air at a number of pressures will be passed through a number of different lengths and diameters of nylon tubing to confirm if there are any relationships that can be used to

include a length factor to a leak characterization chart. Further work could be done to extend this study to other materials.

3.3.3 Distance from the Leak

As part of the standard operating procedure when using the UE Systems Ultraprobe 9000 the recommended distance from the leak to the scanner is between 12” and 15”, this is equated to leak rates that are included in their “Compressed Air Ultrasonic Leak Guide”. It is not always possible, or practical, to be at this distance for a number of reasons. Pipe work may inhibit your access to the leak at the distance required, the leak may be at a height that is out of reach without specialized equipment or competing ultrasounds that you cannot shield from the scanner may make it preferable to carry out scanning closer to the leak site. The effect of measuring the ultrasonic level from set distances from the leak source will be examined and if the results allow an offset value or multiplier will be included in the leak characterization charts.

3.3.4 Directionality

Early experimental work for this study when learning about the scanning device indicated that the ultrasonic sound level was not constant from every angle at a set distance. Further testing showed that there appeared to be a significant drop in sound level along the axis of the flow. This was an important finding, as a characterization chart will only be useful if the user can be confident that their measured ultrasonic sound level corresponds with the chart. The variance in ultrasonic sound level at a number of angles relative to the leak site will be measured to establish if there is a pattern to the level of ultrasonic sound at any point around the leak. If a pattern is found to exist, it will be built into the characterization chart or leak detection methodology.

3.4 Ultrasonic Leak Detection Procedure

3.4.1 UE Systems “Guess-timator” Chart

The UE Systems Ultrasound 9000 and 10000 are currently at the leading edge of ultrasonic leak detection and are used in conjunction with a “Guess-timator” chart that is included as part of the “Compressed Air Ultrasonic Leak Guide” that is available with the scanner. The chart gives a very rough approximation of leak rate at a given pressure and decibel reading as shown in Table 3.1 and does not take account of any other factors.

If the “Guess-timator” chart is displayed as a graph, as shown in Figure 3.1, we can see that the profile of the ultrasonic sound level to volume flow rate is quite erratic. Although the general trend of the graph shows that as the pressure increases the volume flow rate for a given ultrasonic sound level also increases, there are a number of anomalies that do not follow the expected profile.

It was developed by measuring a selection of leak rates, for specific decibel readings, and a variety of different sized leaks, at line pressures of 10, 25, 50, 75 and 100 psi(g). These leak rates were combined to give a typical leak rate for a specific decibel reading at a known system pressure. Although this does help to give some idea of a leak rate, there are obvious dangers in using this to estimate the loss from a compressed air system, especially if the number of leaks is small. As a result UE Systems themselves recommend a “discount factor” of about 50%.

DIGITAL READING	100 PSIG	75 PSIG	50 PSIG	25 PSIG	10 PSIG
10 dB	0.5	0.3	0.2	0.1	0.05
20 dB	0.8	0.9	0.5	0.3	0.15
30 dB	1.4	1.1	0.8	0.5	0.4
40 dB	1.7	1.4	1.1	0.8	0.5
50 dB	2.0	2.8	2.2	2.0	1.9
60 dB	3.6	3.0	2.8	2.6	2.3
70 dB	5.2	4.9	3.9	3.4	3.0
80 dB	7.7	6.8	5.6	5.1	3.6
90 dB	8.4	7.7	7.1	6.8	5.3
100 dB	10.6	10.0	9.6	7.3	6.0

NOTES:
ALL READINGS ARE COMPENSATED FOR ATMOSPHERIC PRESSSURE.
All readings were taken at 40 kHz.

Table 3.1, UE Systems Guess-timator chart for the UP 9000/10000, dB v CFM.

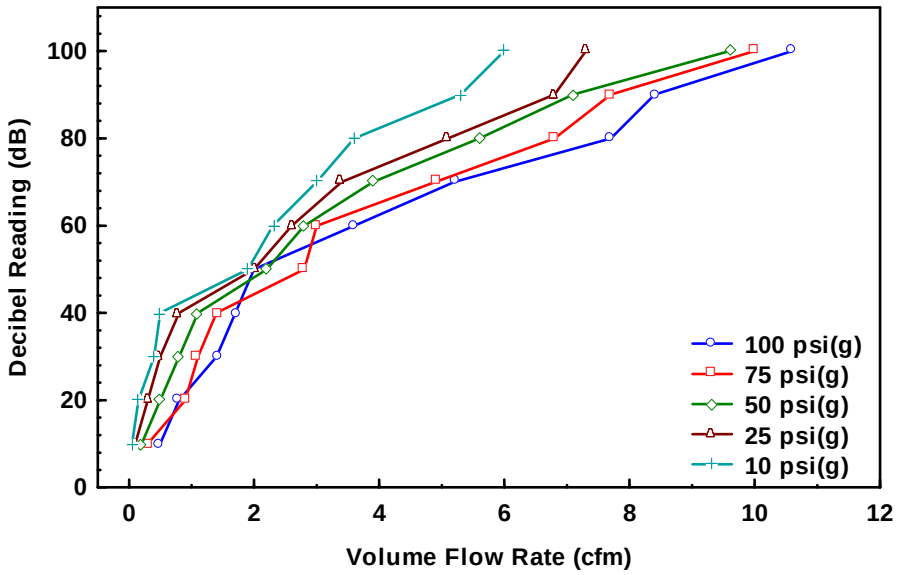

Figure 3.1, Graph of UE Systems Guess-timator chart for the UP9000/10000, showing the ultrasonic sound level for a volume flow rate at 10, 25, 50,75 and 100 psi(g)

3.4.2 Development of Leak Characterisation Chart

The current “Guess-timator” Chart is a very rudimentary tool to be used as an indication of the level of leak rates within an industrial plant. Following the review of the factors affecting the flow rate and corresponding ultrasonic sound level this study will aim to develop a more advanced leak characterisation chart, or charts, that will include these factors in an integrated fashion that is significantly more accurate for a range of situations while still being relatively straightforward to use.

3.5 Theory of Turbulent Flow from a Round Jet

One of the fundamental elements to this study is the understanding that ultrasound is generated by turbulence created by flow from a leak. It is therefore important that time is taken to explain how the turbulence is generated and how this relates to the profile of ultrasound being measured at the leak site.

The turbulence generated at a leak site most closely resembles a turbulent jet, and for this study the closest approximation is the round or symmetrical jet as shown in Figure 3.2. It is a combination of normal and shear stresses that are generated as the flow separates from the surface of the pipe and within the jet, as ambient air and the convoluted edge of the jet interact. It can be seen that as the axial distance increases the jet decays and spreads as the influence of the flow from the nozzle decreases. It becomes self-similar at around 30 diameters from the nozzle, which means that even beyond the influence of the source of the jet the turbulence continues to spread in the same manner. The spreading of the jet is caused by entrainment of the ambient air at its convoluted outer edge which represents the interface between fluid filled with vorticity and the external, irrotational fluid.

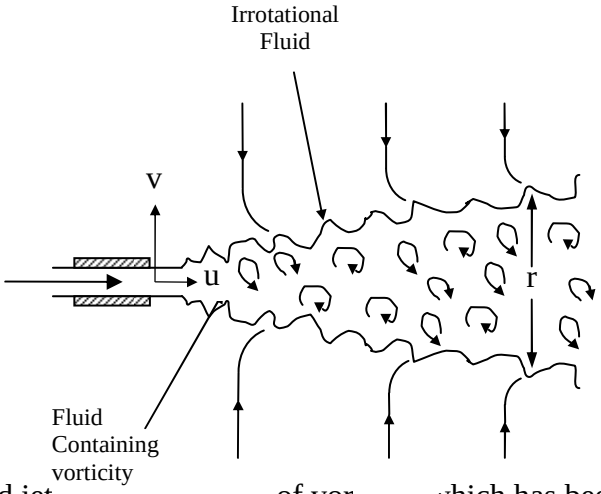

Figure 3.2, A round jet of vor which has been stripped off the inside of the nozzle and is then swept downstream. (Davidson, 2004)

As is discussed in Pope (2000), when a steady air flow from a nozzle exits into the atmosphere, which is stationary beyond the influence of the jet, the flow is steady and symmetrical. As a result, the developing turbulence depends on the axial and radial coordinates (x and r), but is independent of time and the circumferential coordinate, θ. The fluctuating velocity components in these coordinate directions are denoted by *u*, *v*, and *w*.

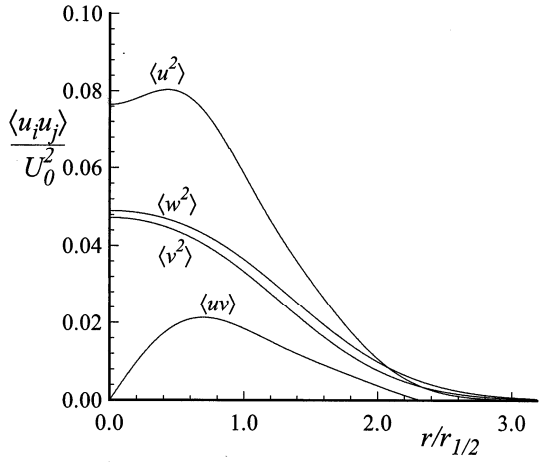

Figure 3.3, Profiles of Reynolds stresses in the self-similar round jet: curve fit to the LDA data of Hussain *et al.* (1994). Pope (2000).

In Figure 3.3, $\langle u^2 \rangle, \langle v^2 \rangle$ and $\langle w^2 \rangle$ are the normal stresses, and $\langle uv \rangle$ is the shear stress for the flow from the jet. As the flow is symmetrical and θ equals zero, $\langle uw \rangle$ and $\langle vw \rangle$ are zero.

When $u_i u_j / U_0^2$ is plotted against $r / r_{1/2}$, it can be seen that the magnitude of the Reynolds stresses varies. The axial component of the normal stresses, $\langle u^2 \rangle$ is highest at $r / r_{1/2}$ equals 0.5 (approx) with a slight reduction at $r / r_{1/2}$ zero, with the radial, and circumferential stresses, $\langle v^2 \rangle$ and $\langle w^2 \rangle$ respectively, peaking at zero.
These stresses decay to zero on the $u_i u_j / U_0^2$ axis towards the edge of the jet. The magnitude of the shear stress component of the flow is zero in the central axis, and is lower than the normal stress components at its peak, before also decaying to zero towards the edge of the jet.

The dominant normal stress and the shear stresses peak at $r / r_{1/2} \approx 0.5$, therefore it can be concluded that the highest level of turbulence is in this region, and as the distance from the source increases additional irrotational air is drawn into the jet increasing its girth.

3.6 Acoustical Theory

3.6.1 Acoustical Refraction in a Jet

Studies carried out by C.K.W. Lam & L. Auriault showed that a radial gradient in gas flow velocity leads to acoustic refraction, as depicted in Figure 3.4. This shows a wave front at AB which, at a time t later, has moved to A´B´. This assumes that the component at point B travels at a faster velocity than at A, so that the wave will refract or bend outwards. This results in a region of low intensity sound intensity or “cone of silence” along the axis of the flow, which accompanies divergence of the sound field.

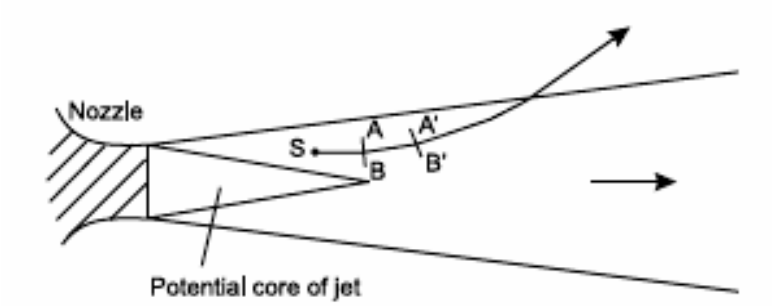

Figure 3.4, The possible refraction effect on an acoustical wave in a flow from a jet (Tam and Auriault)

This effect helps to explain the fall in ultrasonic sound level in the central flow axis and further analysis in the experimental studies will look to profile the directionality of the ultrasonic sound level around a leak.

3.6.2 Inverse Distance Law

Sound Intensity is the sound power (Watts) flow through a unit area. The intensity level L_1 for a sound wave whose intensity at a specified point is I (W/m^2) is defined as

$$L_1 = 10 \log_{10} \frac{I}{I_0} \tag{3.1}$$

L_1 is expressed in dB with reference to I_0.

This can be demonstrated when a single sound source propagates uniformly in all directions in the form of an expanding spherical shell as shown in Figure 3.5.

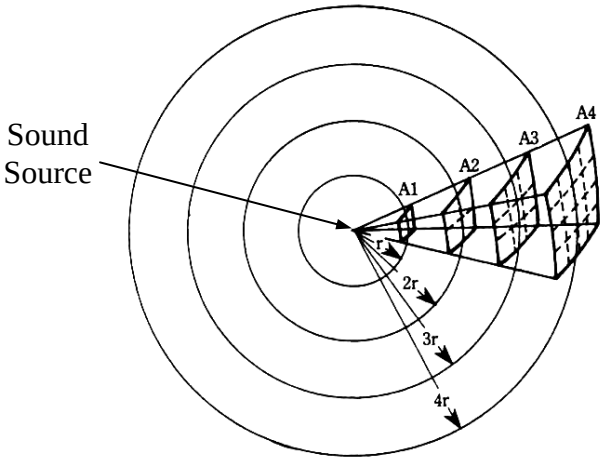

Figure 3.5, Spherical propagation of a pulse

Using the equation for the surface area of a sphere

$$A = 4\pi r^2 \tag{3.2}$$

It follows that if

$$A_1 = 4\pi r_1^{\,2} \text{ and } A_2 = 4\pi r_2^{\,2}$$

and, the sound power is constant, then substituting I_0 with A_1, and I with A_2 in

$$L_2 = L_1 - 10\log_{10}\frac{I}{I_0} \tag{3.3}$$

where L_2 is the new sound level and L_1 is the starting sound level, gives

$$L_2 = L_1 - 10\log_{10}\frac{A_2}{A_1} \tag{3.4}$$

Substituting A_1 and A_2 we get

$$L_2 = L_1 - 10\log_{10}\left(\frac{4\pi r_2}{4\pi r_1}\right)^2 \quad (3.5)$$

which can be simplified to

$$L_2 = L_1 - 10\log_{10}\left(\frac{r_2}{r_1}\right)^2 \quad (3.6)$$

This can be rewritten as

$$L_2 = L_1 - 20\log_{10}\left(\frac{r_2}{r_1}\right) \quad (3.7)$$

Equation (3.7) is known as the inverse square or, inverse distance law.

This law is used to calculate the sound level at different distances from a sound source. It is designed for use in perfect conditions for example an anechoic chamber and is predominantly used in the audible sound range.

In enclosed spaces, and in the audible sound range, as the distance from the source increases, the level of direct sound approaches the level of reverberant sound. The distance at which this occurs is called the critical distance and beyond this distance the sound level will not reduce further until the sound begins to attenuate. Until this distance is reached, the inverse distance law is valid. As is shown in

Figure 3.6, the inverse square law is applicable at short distances in both the audible sound range and the ultrasonic sound range. However, at greater distances, reverberation in the audible sound range, and more likely, attenuation in the ultrasonic sound range, render the law invalid.

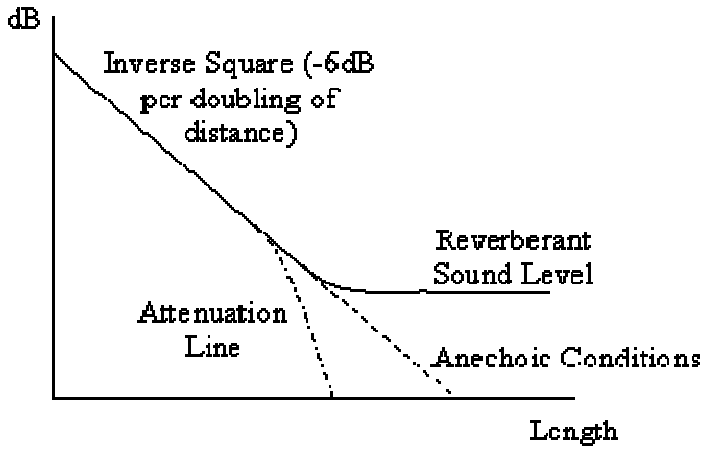

Figure 3.6, Graph showing how the reverberant sound level in the audible sound range and attenuation in the ultrasonic sound range affect the Inverse Square Law.

The validity of the inverse distance law, when quantifying compressed air leaks by ultrasonic detection, will be examined to determine how the recorded level of ultrasound is affected by reverberation and attenuation.

3.7 Critical Flow Theory

A common assumption when carrying out compressed air leak surveys is that as pressure increases the flow rate of the air will also continue to rise proportionately. However this takes no account of the critical flow effect.

Critical flow occurs when a gas flowing through an orifice reaching sonic velocity. When the ratio of an upstream pressure to a downstream pressure reaches a specific value the volumetric flow rate is unable to increase any further.

This pressure ratio is calculated using

$$p_1 / p_2 = \left[(k+1)/2\right]^{k/(k-1)} \tag{3.8}$$

For air k = 1.4, this gives,

$$p_1 / p_2 = 1.89 \tag{3.9}$$

If p_2 is atmospheric pressure, then using the value from equation (3.9) we get

$$p_1 = 1.89 \times 1.01 = 1.91 \text{Bar}$$

This shows that at standard conditions of temperature and pressure, critical flow will occur at 1.91 Bar (absolute).

The validity of the critical flow effect with respect to compressed air leaks will be explored in the course of this thesis.

4 Test Rig Design

4.1 Test Rig Elements

4.1.1 Overview

A test rig was required to enable accurate measurement of line pressure, leak pressure and the volume flow rate of compressed air through a variety of leak types, to allow comparison to be drawn between dB readings at various exit conditions. It was important that the rig was designed with repeatability in mind again to ensure comparison between the various experiments was possible. There were several elements to the rig, as listed below.

1) Receiver tank with regulator and pressure gauge to control and measure the entry pressure.
2) Rectutest flow meter and rotameters for lower flow rates.
3) Manifold used for connection of various tube diameters.
4) Chamber used for mounting of discs and pressure transducer.
5) Orientation board to ensure accuracy of the angle of the ultrasonic leak detector relative to the leak.

The schematic in Figure 4.1 shows how the test rig was assembled and the following sub sections describe each of the elements that made it up.

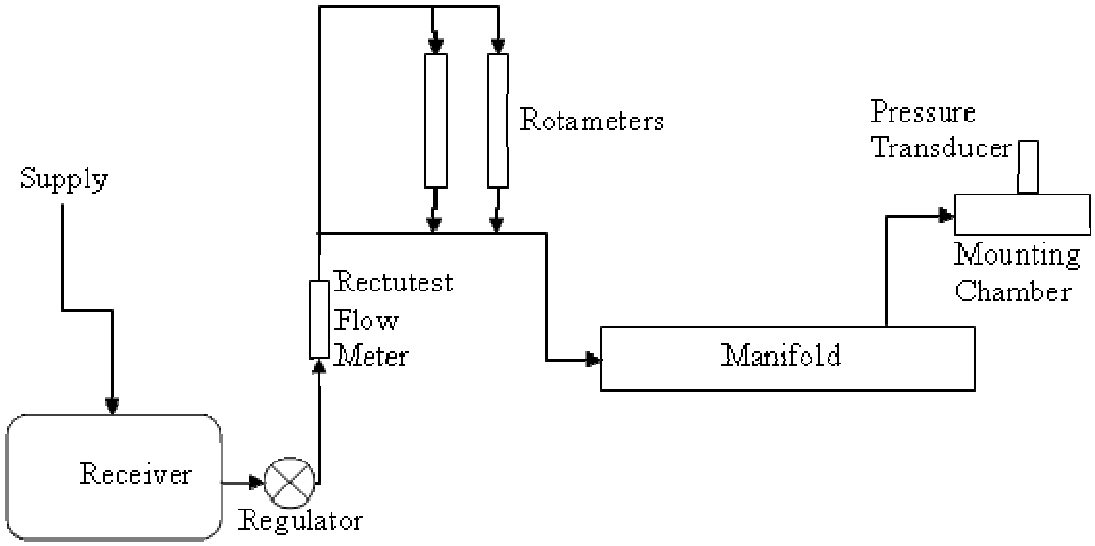

Figure 4.1, Schematic of the test rig.

4.1.2 Receiver Tank with Air Regulator

A receiver tank was required to stabilise the line pressure of air through the rig to compensate for compressor loading and unloading and also additional use of the lab compressed air. A 100 Litre tank was obtained for this purpose. Ideally a larger tank would have been used but sourcing such a tank with the budget available was not possible. The tank sourced reduced flow fluctuations and assisted with reducing the settling time of the system (Refer to Figure 4.2). A pressure regulator (shown in Figure 4.3) with a pressure gauge was attached onto the demand side of the receiver to allow the flow to be accurately controlled and to enable the receiver to be maintained at as high a pressure as possible.

Figure 4.2, 100L Air Receiver

Figure 4.3, Air Regulator

4.1.3 Manifold

A manifold was positioned in the rig to allow various configurations that required different connectors to be set-up without requiring changes to the test rig. This allowed experiments to be revisited at a later time with minimal disruption and with the knowledge that there would be no variations to experimental conditions. (Refer to Figure 4.4) Isolator valves were situated at several points on the manifold (as shown in Figure 4.5) to allow changes to be made to the set-up without the need to depressurise the rig between experiments.

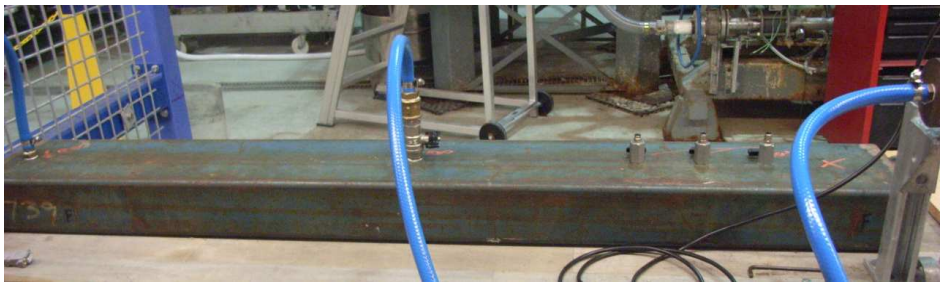

Figure 4.4, Manifold with inlet from supply and various outlets.

Isolator Vales

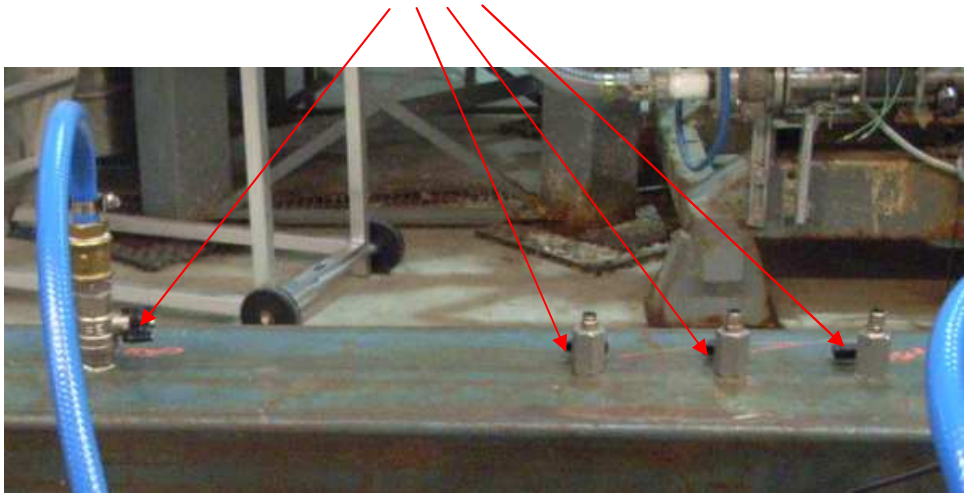

Figure 4.5 , Manifold with Isolator valves identified.

4.1.4 Test Piece Mounting Chamber

The mounting chamber (as shown in Figure 4.6) consisted of a metal tube with a connector at one end for the inlet and a flange at the other to allow placement of metal discs with orifices of varying sizes and geometries to simulate various leaks. There was also a port on the side of the chamber to allow a 10 Bar pressure transducer to be attached.

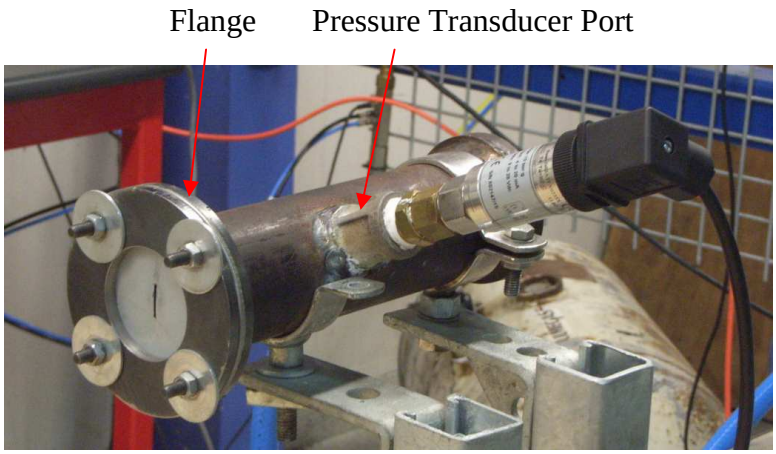

Figure 4.6, Test Piece Mounting Chamber

4.1.5 Orientation Board

A board with Markings from -90° to 90° was designed, with 0° being in the centre and line with the flow. Circumferential markings were spaced so that the end of the rubber focusing probe attached to the Ultraprobe was positioned at 100mm, 150mm and 300mm from the leak as can be seen in Figure 4.7.

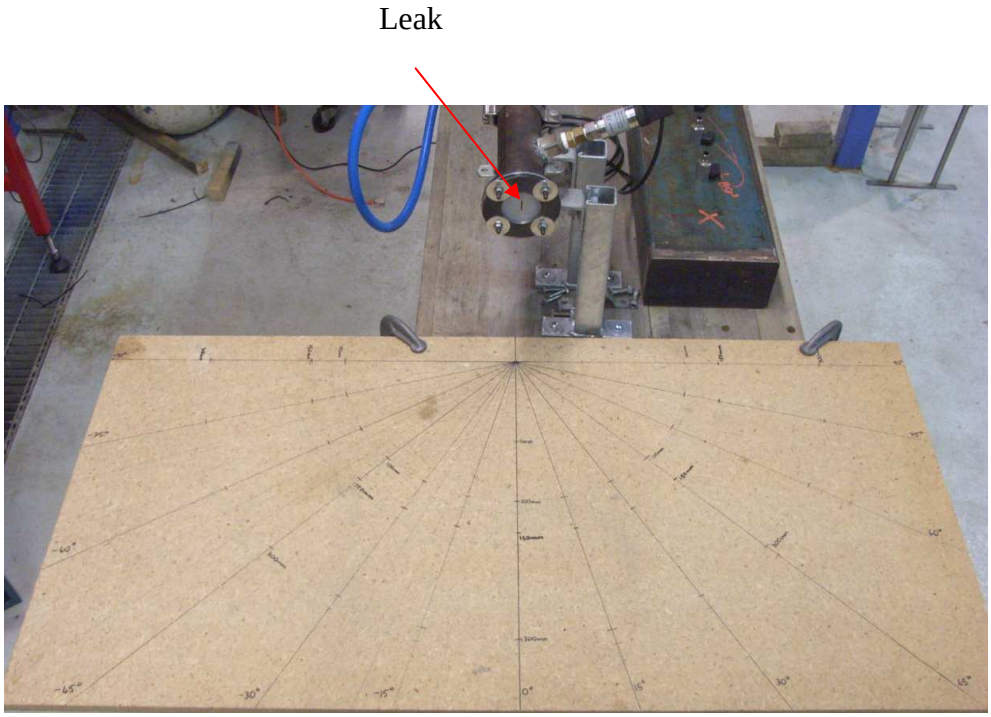

Figure 4.7, Orientation Board with markings for positioning of Ultraprobe.

4.2 Instrumentation

4.2.1 Flow Measurement

Flow measurement was carried out in-line between the receiver and the manifold using two different devices. One, the Rectutest RT02 was used for the higher flow experiments. This was a useful device as it was capable of electronically logging flow, pressure and temperature simultaneously using an in-line flow cell and control unit to calculate and display the flow rate. This allowed monitoring of the stability of the flow over the duration of the experiment. However there was a minimum flow threshold, below which the Rectutest was unable to provide a flow rate under certain circumstances. This generally occurred when small diameter tubing was used and the back pressure was significant.

The Rectutest meter is able to measure volume flow rate, pressure and temperature in a number of units, this study was performed using standard m^3/h for flow, Bar for temperature and °C for temperature.

For the lower flow rates two Dwyer rotameters have been used, one, 0 – 200 scfh, the other 0 – 50 scfh. These could be isolated from the system to ensure that they didn't affect the flow and also to allow the manifold to be charged in as little time as possible. The Dwyer Rotameters are shown in Figure 4.8, and the Rectutest RT02 control unit and flow cell are shown in Figure 4.9 andFigure 4.10 respectively.

Figure 4.8, Dwyer Rotameters.

Figure 4.9, Rectutest RT02 Control Unit.

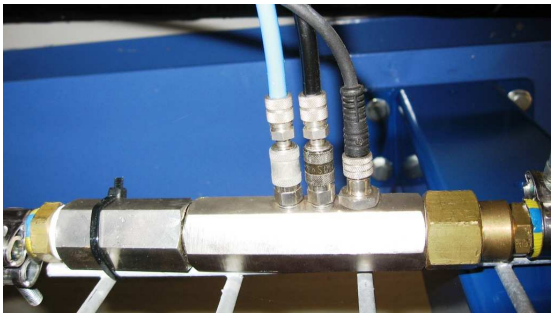

Figure 4.10, Rectutest RT02 Flow Cell.

4.2.2 Pressure Measurement

Pressure was measured at two points in the test rig. Firstly at the exit of the receiver by means of a pressure gauge on the regulator showing the system pressure, and also at the mounting chamber by means of a 10 Bar pressure transducer. (as shown in Figure 4.11), this was connected to a data logger that was continuously recording the pressure over the duration of each experiment.

Figure 4.11, 10 Bar Pressure Transducer

4.3 UE Systems Ultraprobe 9000

The Ultraprobe 9000 (Refer to Figure 4.12) is the ultrasonic leak detector that I used for my study. It can be used for Electrical Inspections, detecting corona, tracking and Arcing, Mechanical Inspections, detecting worn bearings, cavitation and steam trap faults, and the area that I have been investigating, Leak Detection. The Ultraprobe device uses patented trisonic transducers (as shown in Figure 4.13) to detect vibrations with a sensitivity which allows it to detect a 0.127mm (0.005”) diameter leak at 0.34 Bar (5psi) from a range of 15.24m (50’). The threshold for leak detection is 1×10^{-2} std. cc/sec to 1×10^{-3} std. cc/sec depending on the leak configuration. This exceeds the ASTM Standard Test Method for Leaks Using Ultrasonics. (UE Systems and ASTM Standard E 1002 – 05).

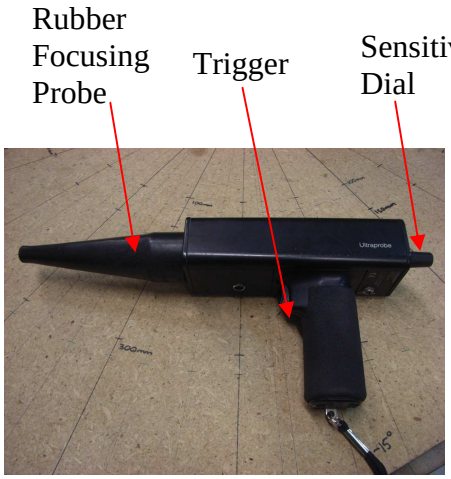

Figure 4.12, Ultraprobe 9000

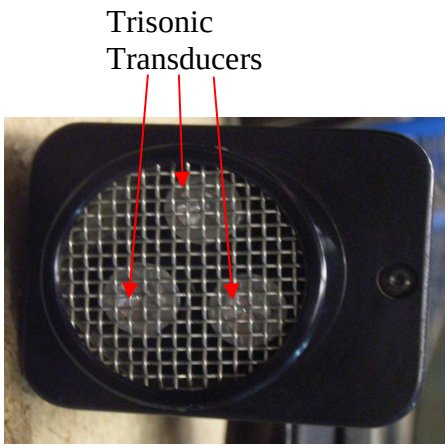

Figure 4.13, Piezoelectric Module

The Ultraprobe device is switched on using a trigger and the frequency and sensitivity are adjusted using a small dial below the viewing window. Headphones are generally worn to listen to any leaks and the high frequency noise is heterodyned to allow it to be heard by the human ear. As can be seen in Figure 4.14, the frequency is displayed on the right hand side and for this study was kept fixed at 40kHz, (however for other applications this may be different), the dB reading is displayed as a number on the left hand side of the display with the strength of the signal below as a dark bar. The sensitivity dial is in essence a volume control for the device to allow the signal to be picked up at the low and high ends of the spectrum respectively.

Figure 4.14, Ultraprobe 9000 Display

5 Experimental Procedures

5.1 Leak Sample Preparation

5.1.1 Open Ended Nylon Tubing

Initial experimentation using open ended Nylon Tubing of outside diameter 10mm and 6mm and 4mm (as shown in Figure 5.1) was carried out. Each diameter of tubing was cut to 1m, 2.5m, 5m, 7.5m and 10m. This was done using a specialized tube cutter to give a square cut and each section of tubing was checked against a set square to ensure uniformity. The full dimensions of the tubing are given in Table 5.1.

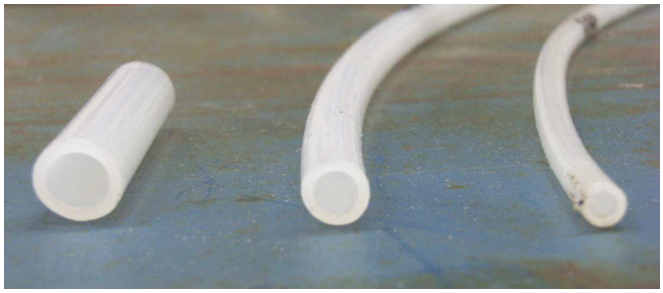

Figure 5.1, Examples of the three diameters of nylon tubing used in experiments

Table 5.1, Lengths of nylon tubing for each diameter

	OD (mm)	ID (mm)	Tube Length (m)					
Open Ended Tube	4.0	2.5	1.0	2.5	5.0	7.5	10.0	25.0
	6.0	4.0	1.0	2.5	5.0	7.5	10.0	25.0
	8.0	6.0	1.0	2.5	5.0	7.5	10.0	25.0

5.1.2 Slot and Round Hole Leak Discs

The Discs were cut from Mild Steel using a Trumpf TruLaser 5040 machine to ensure maximum accuracy. Laser cutting was used due to its high level of accuracy (+/- 100 Microns), however, as the sizes required for the test pieces were

so small, even a minor variation in cut size could result in a noticeable variation in the test results. The dimensions were checked using a microscope at a magnification factor of 6.4x to verify their accuracy. The results of the check showed that the test pieces that were intended to have a 0.5mm width slot, had 0.625mm slots, a difference of 0.125mm. Magnification also identified discrepancies in the geometry of a number of the slots in the test pieces as the corners of them were round rather than square. This meant that exact measurement of these test pieces was not possible and could still lead to minor variations in the test results. Each disc was 100mm diameter, with 4 symmetrical holes cut to allow them to be bolted to the mounting chamber. It was important that the mounting holes were in the same position relative to the leaks on each test piece to ensure that the leak orientation was the same for each test. of various geometries and were designed to mimic leaks from specific hole sizes and shapes. Three examples of the discs are shown in Figure 5.2 -Figure 5.4. The dimensions of the discs are given in Table 5.2.

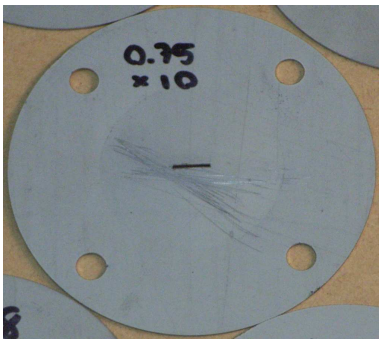

Figure 5.2, Disc with 0.75mm x 10mm slot

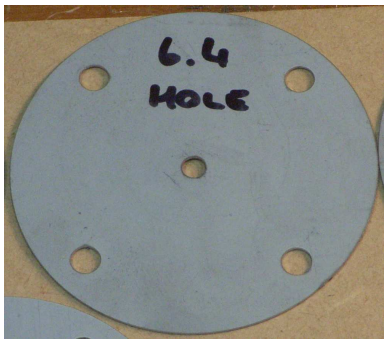

Figure 5.3, Disc with 6.4mm diameter hole

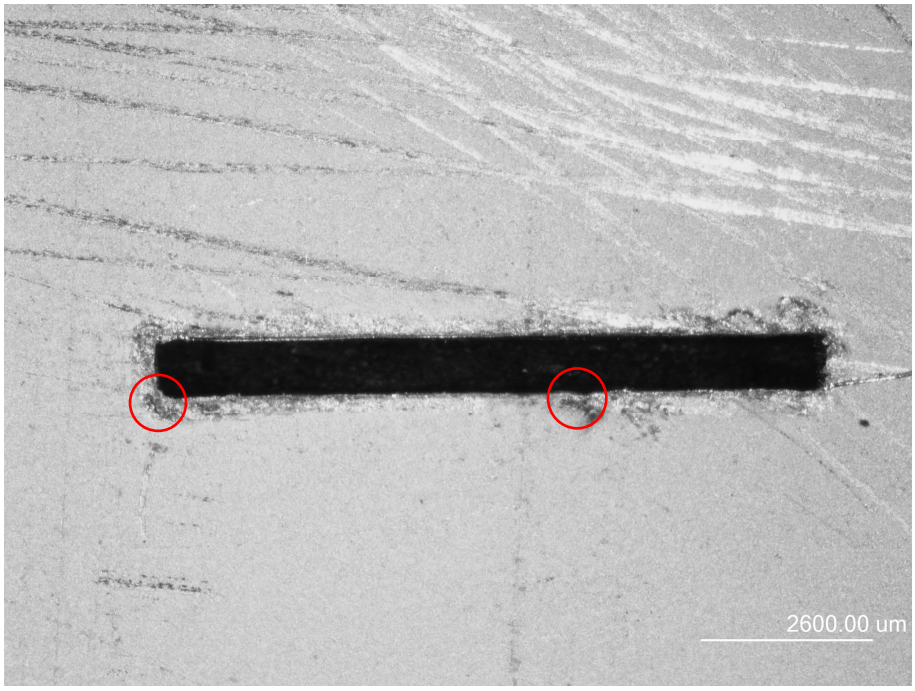

Figure 5.4, 0.75mm x 10mm slot magnified 6.4x showing a rounded corner and imperfections along the cut.

Table 5.2, Dimensions of orifice geometries in mild steel discs.

		Disc Thickness (mm)	Hole Diameter (mm)									
Mild Steel Discs	Round Holes	0.6	1.0		1.6		3.2		6.4			
		2.0	1.0		-		-		6.4			
	Slots	Disc Thickness (mm)	Width (mm)	Length (m)								
		0.6	0.5	-	5.0	-	-	10.0	15.0	-	30.0	-
		0.6	0.8	-	5.0	-	-	10.0	15.0	20.0	-	-
		0.6	1.0	2.0	5.0	-	8.0	10.0	15.0	-	-	32.2
		0.6	2.0	-	5.0	7.5	-	-	-	-	-	-
		2.0	1.0	-	5.0	-	-	-	15.0	-	-	-

5.2 Experimental Rig Set-up

5.2.1 Leak set-up with Nylon Tubing

One end of the Nylon Tubing was attached to the Manifold by a straight adapter, the end being used for testing was secured to a bracket with the exit in line with the 0° line on the orientation board and with the end of the tube in line with the 90°/-90° line as shown in Figure 5.5.

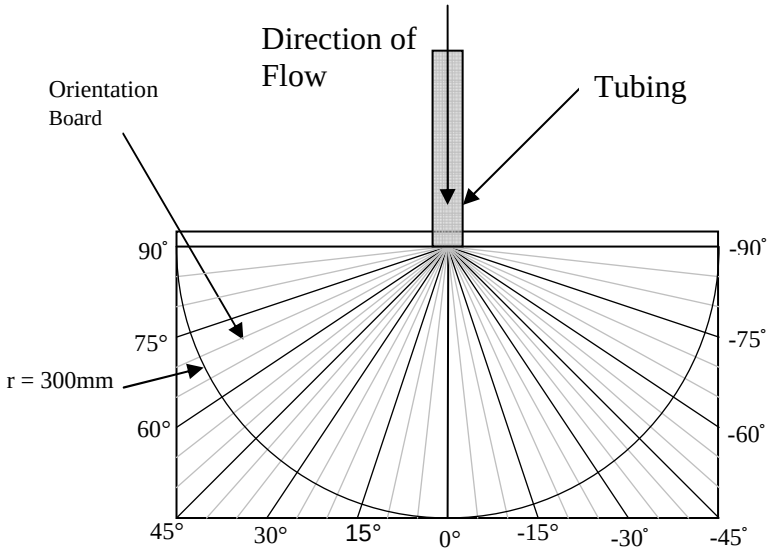

Figure 5.5, Top view of tubing direction relative to orientation board (Not to scale)

5.2.2 Leak Set-up for discs

The discs were mounted onto the chamber as shown in Figure 5.6 andFigure 5.7 and were sandwiched between a gasket and a 6mm thick steel ring that was bolted onto the flange. The orientation of the slot leaks was checked with a set square and spirit level to ensure the leak was horizontal to the board.

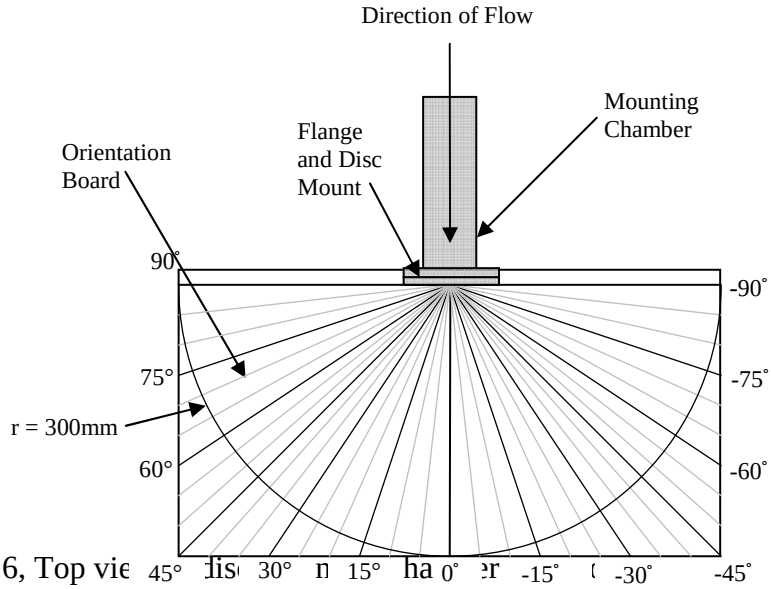

Figure 5.6, Top view of disc mounting chamber relative to orientation board (Not to scale)

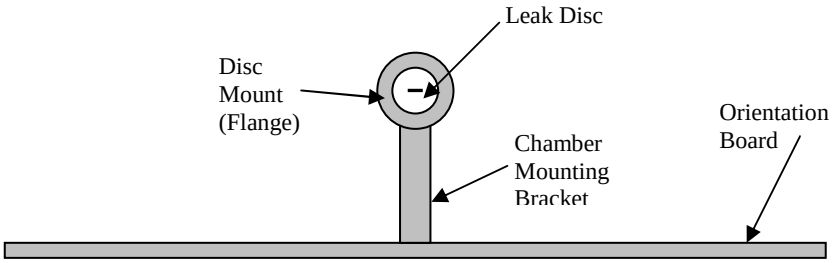

Figure 5.7, Front view of disc mounting chamber and leak disc relative to orientation board. (Not to scale)

5.3 Instrumentation Accuracy

5.3.1 Pressure Measurement

The Druck PTX1400 pressure gauge used for measuring the leak pressure has a typical accuracy of 0.15%.

5.3.2 Flow Measurement

The Rectutest RT02 has measuring accuracy of +/- 2.5% of the measurement value. With a maximum permissible operating pressure of 10 Bar.

The Dwyer Rate-Master RMC flowmeters used for the lower pressure experimentation were accurate to within 2% of full scale.

5.3.3 Ultraprobe

The Ultraprobe 9000 is calibrated to ASTM standard 1002 – 05. with sensitivity validation undertaken on a regular basis to ensure consistent results. This consisted of setting the ultraprobe to a specific sensitivity and frequency. Then it was positioned at a set distance from the warble tone generator and the decibel level measured.

6 Experimental results

6.1 Overview

For this study two leak type groups were investigated. The first leak type group consisted of open ended tubing, while the second leak type group consisted of a range of 100mm diameter mild steel discs and were divided into two types, round holes and slots. The dimensions of each of these groups can be located in tables 5.1 – 5.4 respectively.

This chapter will present the raw data from each set of tests in graphical and tabular form to show how Pressure, Tubing Length, Tubing Diameter, Leak Shape and Leak Size impact on leak rate and dB sound level and how the distance from the leak, and angle to the leak (otherwise known as angle of approach), of the scanning device also affects the acoustic reading. From these results a new leak characterisation chart will be built up enabling a more accurate loss rate to be estimated when doing compressed air surveys and audits.

The influence of pressure on the volume flow rate and ultrasound level will be tested, and will aim to demonstrate how the critical flow point affects the flow rate in the air line, and the potential impact of this on the level of ultrasound recorded, the impact of normalising the flow will also be examined in this section. The effect of changing the orientation, and distance of the leak detector to the flow from the leak, on the ultrasonic sound level, will be studied. This will be followed by a study of the effect of varying the leak size, geometry and type on dB levels for a number of system pressures.

6.2 Normalisation and Critical Flow Point

6.2.1 Normalising the Flow Rate

The pressure and volume flow rate in a compressed air system are not controlled or measured when conducting an air leak survey using an ultrasonic leak detector. Being able to obtain a relatively accurate volume flow rate for a variety of conditions would be very useful.

The volume flow rate was plotted against supply pressure as shown in Figure 6.1 and shows that, with the exception of very low pressures, the flow rate increases with pressure at a constant gradient for a given diameter of tubing. By normalising the volume flow rate (at standard conditions) with respect to the line pressure as shown in Figure 6.2 we obtain a volumetric flow rate that is uncorrected for pressure. This flow rate changes below the critical flow point, which occurs at a specific pressure, see 6.2.2. Once the supply pressure rises above this, the flow rate is constant at any point in the system. This normalised flow can be converted back to the actual volume flow rate at any point in the distribution network, if the atmospheric pressure and supply pressure at that point are known. From here on the volumetric flow rate will be the uncorrected flow rate in the distribution network unless otherwise stated.

6.2.2 Critical Flow

Critical flow occurs when there is a significant difference between the upstream pressure and downstream pressure. As is discussed in 3.7, for critical flow to exist the ratio between the exit pressure at a leak and the atmospheric pressure must be greater than 1.89. Thus the pressure at which critical flow occurs is around 1.91 Bar_a.

To confirm how the results from this study compared with the theoretical value above, a graph of volumetric flow rate as a function of supply pressure (gauge) was plotted for three air lines of ID 2.5, 4.0 and 6.0mm respectively. Each plot changed in gradient at approximately the same pressure, as shown in Figure 6.1, this was the

critical flow point. The graph was re-plotted, uncorrected for pressure and the transition region to critical flow is much more obvious, see Figure 6.2. As there were very few data points, the point at which the transition took place is unable to be determined. Figure 6.3 shows the same results but also includes additional data collected at lower pressures for the same set of tests. By applying a best fit line to the new data a more complete representation of the transition to critical flow has been obtained. This shows that experimentally the transition to critical flow occurred close to the theoretical pressure calculated of 1.9 Bar_a.

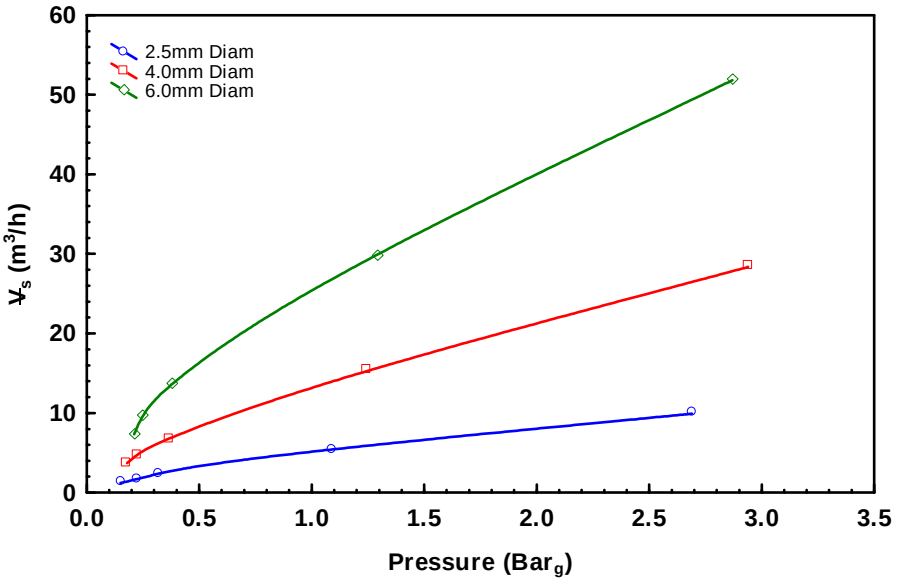

Figure 6.1, Standard Flow rates through 1m lengths of nylon tubing of 2.5, 4.0 and 6.0mm diameter.

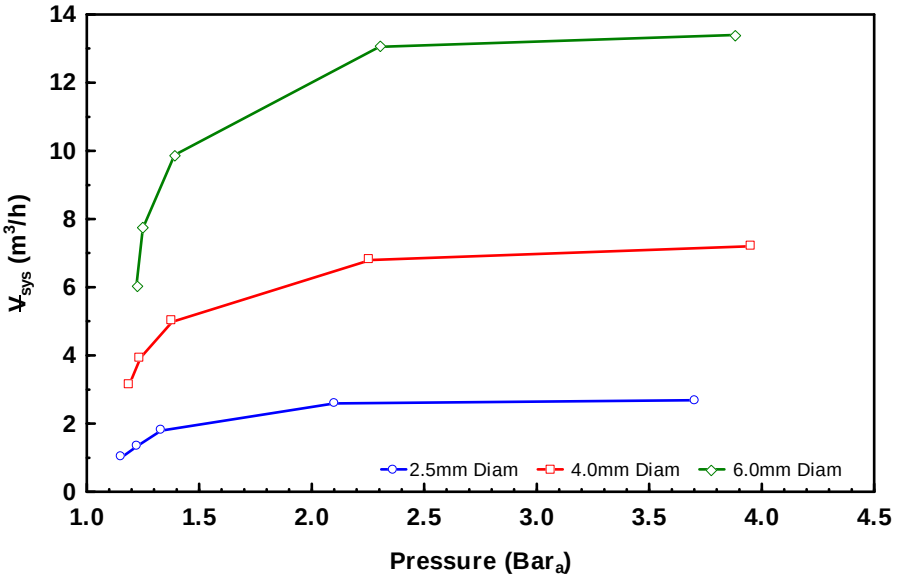

Figure 6.2, Volumetric flow rates, through 1m lengths of nylon tubing of 2.5, 4.0 and 6.0mm diameter, normalised for pressure.

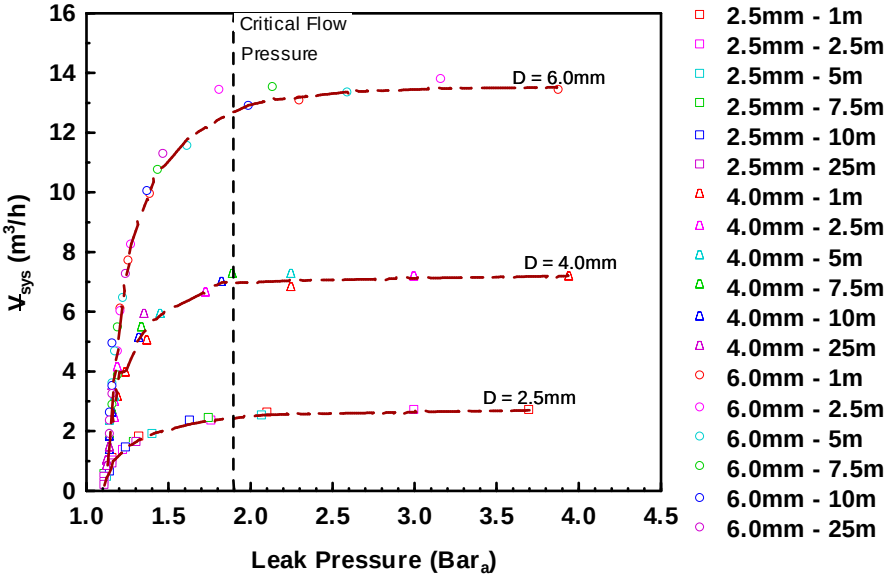

Figure 6.3, Volumetric flow rates for tubing of various lengths at diameters of 2.5, 4.0 and 6.0mm highlighting the critical flow pressure.

6.2.3 Pressure Effect on Decibel Reading

The ultrasonic sound level was measured at a range of pressures for two different leak types. The dB readings obtained were plotted against the pressure to see how the ultrasonic sound level varied with pressure.

Figure 6.4 shows that for a 1mm x 10mm slot, as the leak pressure increased, so to did the Ultrasonic sound level. Initially, at low pressures, the ultrasound level increased rapidly as the flow became more turbulent, when the pressure was increased above the critical pressure, the increase in the ultrasound level slowed as the pressure was increased. The profile of the plot is very similar to that of the normalised volumetric flow rate against leak pressure, Figure 6.3. This indicates that the critical flow point influences the level of ultrasound at a leak. The same study was carried out for a 2.5m length of 4mm tubing, as shown in Figure 6.5. The supply pressures ranged from 1.21 Bar_a to 7.01 Bar_a, but the leak pressures were significantly lower due to the pressure drop through the tubing. Figure 6.6 shows that the profile of the leaks was very similar in the range of pressures that were covered, and the additional results in Figure 6.7 show how the profile was consistent at different sizes of leak, there were two cases where the ultrasound level did not appear to have stabilised at the same point, however this was likely to have been in part, a problem with the resolution of the profile caused by the lack of data points. In most cases the level of ultrasound stabilised at approximately 4 Bar_a, above this leak pressure the level of ultrasound does not significantly increase.

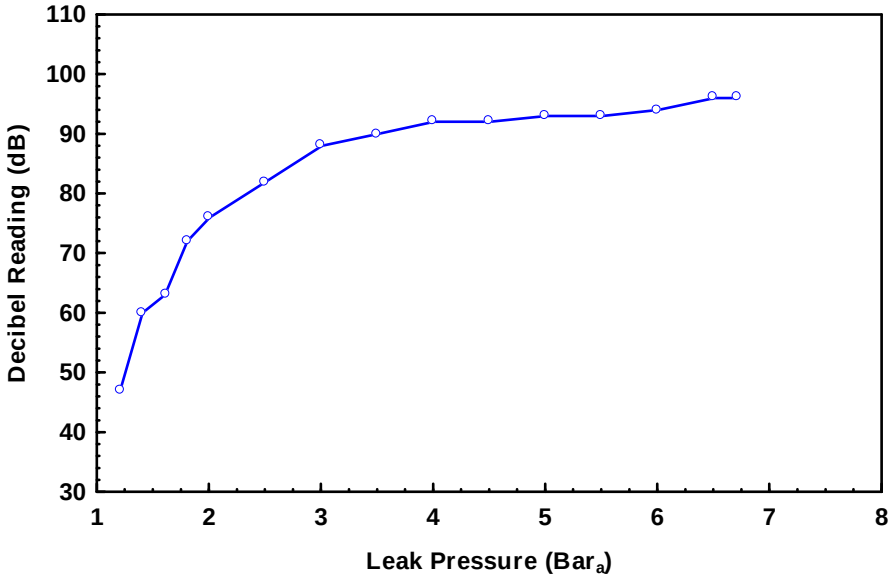

Figure 6.4, Ultrasound level at a distance of 0.3m from a rectangular leak of 1mm x 10mm at range of leak pressures.

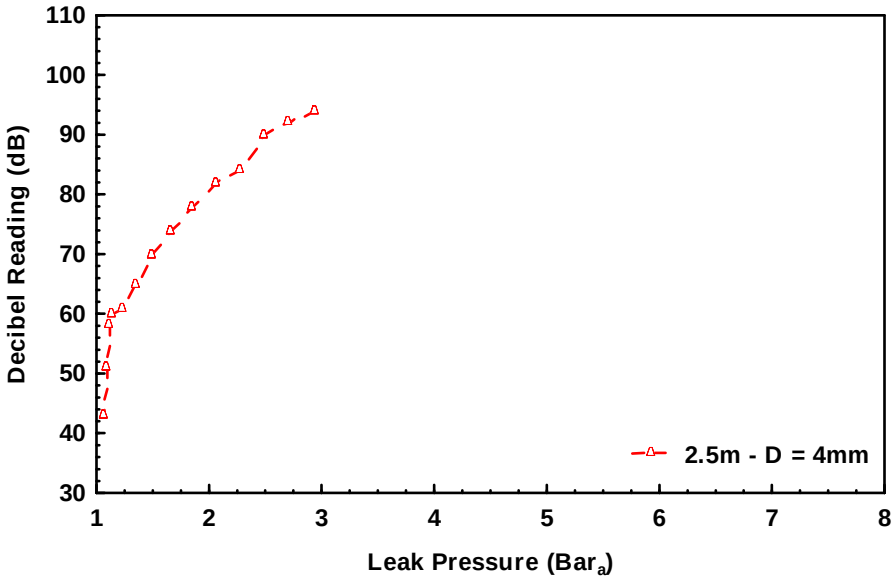

Figure 6.5, Ultrasound Level at a distance of 0.3m from open ended tubing of 4mm diameter and 2.5m length, for a range of leak pressures.

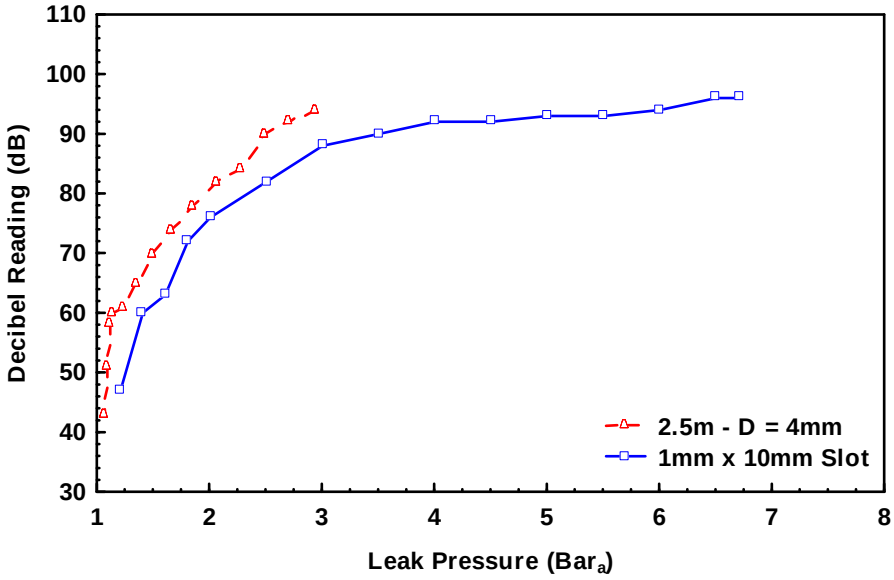

Figure 6.6, Comparison of Ultrasound profile for a 2.5m length of 4mm diameter tubing and a 1mm x 10mm slot at a range of pressures measured at 0.3m from the leak source.

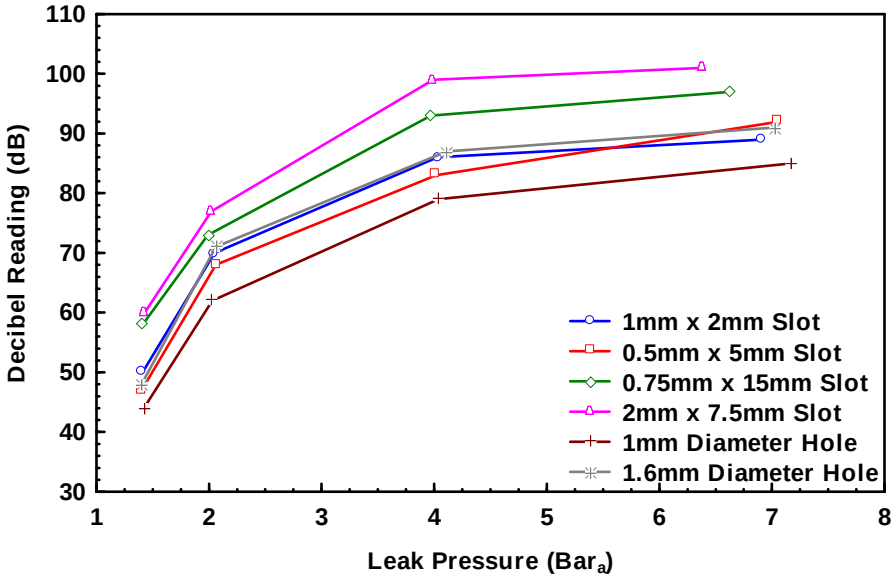

Figure 6.7, Ultrasonic sound levels at a distance of 0.3m from leak source for a variety of geometries over a range of leak pressures.

6.2.4 Summary

This is an important finding in relation to conducting leak surveys as it means that for any given size of leak, once the leak pressure is above 3 Bar$_g$ even though the flow

rate continues to increase linearly, the maximum level of ultrasound will remain approximately the same for that leak. This maximum level of ultrasound will vary depending on the leak size. This highlights the importance of obtaining a good estimate of the leak pressure, as without it the loss rate from any leak may be grossly underestimated. An example of this would be a ¼" pipe at 43psig (3 Bar_g) which leaks 54cfm (92m^3/h) against the same pipe at 87psig (6 Bar_g) which leaks 95cfm (161m^3/h). Although the difference in leak rate is 41cfm (69m^3/h) the difference in ultrasonic sound level will only be 3dB – 4dB.

6.3 Directionality Analysis

6.3.1 Angle of Approach

The angle of approach, (or orientation), of the ultrasonic leak detector to a leak source was tested to confirm if the level of ultrasound detected changed.

Current practice when using the UE Systems Ultraprobe to conduct a leak inspection is to determine where the leak is, stand facing the leak, and then draw back to a distance of approximately 15". Initial investigation for this thesis suggested that the highest level of ultrasound was not directly in line with the source, the reason for this is discussed in 3.6.1.

To study where the highest level of ultrasound relative to a given leak was located, round tubing of 2.5m length and 4mm I.D. was used as a leak source and the variations in dB level relative to the direction of flow measured using an ultrasonic leak detector.

The dB reading was measured at a distance of 0.3m from the leak, at 15° intervals in a 180° arc, from 90° to -90°, with 0° being on the leak axis. A diagram of the set-up can

be located in figure 5.5. The study was carried out for a number of supply pressures at 0.2 Bar intervals, from 1.21 Bar_a to 2.01 Bar_a, and 0.5 Bar intervals, from 2.1 Bar_a to 7.01 Bar_a. Several key findings from the test can be taken from Figure 6.8 which shows the variation of the ultrasonic sound level when measured around the leak. (The pressures used for the plot are the leak pressures which were measured at a distance of 30mm from the end of the tubing and are not supply pressures.)

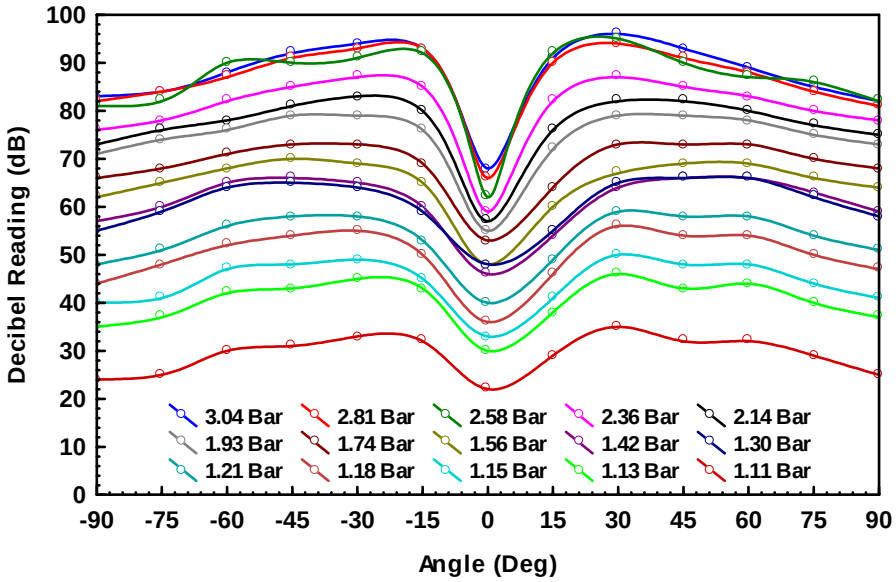

Figure 6.8, Directionality of ultrasound at a distance of 0.3m from the leak for a 2.5m length of 4mm ID tubing at a range of leak pressures.

Figure 6.8 shows two significant features of the ultrasound profile that emerged from the test.

The work of Tam & Auriault, as discussed in 3.6.1 was shown to be valid for the flow of air from a compressed air leak. The ultrasonic sound level dropped off steeply in the central axis of the flow for all the leak pressures included in the study, with a reduction of 25dB to 30dB measured between 0° and 15° at a leak pressure of 3.04 Bar for this type of leak. The extent of the reduction, in this localised region of ultrasound, reduced as the pressure in the system was lowered. The peak ultrasonic sound level was located between 15° and 45° of the central axis of the leak flow, most commonly at about 30°, with the sound level generally reducing by 5dB to 10dB in

the region between 45° and 90° for this leak type. This result was consistent for all pressures included in the test.

The second feature that emerged from the tests was that the ultrasound generated at a round orifice was mirrored on both sides of the central axis in the direction of the flow. This shows that for air flow from a symmetrical leak the ultrasound generated is also symmetrical.

While both of these results are significant as they show that ultrasound is both directional and symmetrical around an axis, some caution is required in how they are applied when conducting a leak survey. It was shown in the tests that the highest level of ultrasound is between 15° to 45° to the direction of the flow from the leak, and that the level of ultrasound is consistent around a symmetrical leak. However, the exact angle to, and geometry of a leak in an industrial situation will seldom be known, and it is therefore important that when conducting a leak survey that the inspector scans in all directions around the leak until the highest level of ultrasound is detected to ensure consistent results. Although the lowest ultrasound level would also give consistent results, the rate of ultrasound increases very rapidly when the detector is not directly in line with the axis of the air flow. The level of ultrasound is relatively consistent across the 15° to 45° region and would therefore limit any potential error.

6.3.2 Correction Factor for In-Line Detection

As it may not always be possible to position the probe at an angle to a leak as a result of operational constraints, a correction factor has been calculated from the results of two types of leak

A correction factor for a 4mm diameter length of tubing was developed by taking the ratio of the highest ultrasound level against the level at 0°, an average of the ratios was used as even at very low pressures there is only a fifteen percent variation in the calculated correction factor, which equates to a variation of 2 – 3dB. There are occasional fluctuations in the ultrasonic sound level, which are due to variations in

flow conditions or leak geometry, but there is a good degree of correlation at pressures above the critical flow level.

Table 6.1, Table showing the ratio between the maximum ultrasonic sound level at a leak and the level at 0° for a 2.5m length of 4mm diameter tubing measured at a distance of 0.3m from the leak.

Pressure	6	5.5	5	4.5	4	3.5	3	2.5	2	1.5	1	0.8	0.6	0.4	0.2
Max dB	96	94	95	87	83	79	73	70	66	66	59	56	50	46	35
dB at 0°	68	66	62	59	57	55	53	48	46	48	40	36	33	30	22
Ratio	1.41	1.42	1.53	1.47	1.46	1.44	1.38	1.46	1.43	1.38	1.48	1.56	1.52	1.53	1.59
Average (6 Bar - 3 Bar)				1.44											

A second correction factor was calculated for an orifice in a pipe with leak pressures of 6 Bar_g and 3 Bar_g. The results gave average ratios of 1.30 for 6 Bar_g and 1.35 for 3 Bar_g. As the ratios were very similar an averaged ratio for the pressures of 1.33 was calculated.

6.3.3 Summary

It has been shown that the angle of approach to a compressed air leak is crucial to obtaining consistent ultrasound levels when conducting a leak survey. Under laboratory conditions the ideal angle was approximately 30°, in an industrial setting, once the inspector has isolated the leak, the leak detector should be drawn across the leak site in all directions to locate the highest decibel reading.

If there is insufficient space at the leak site to manoeuvre the leak detector around the leak to find the maximum reading then if there is a direct line from the leak the appropriate in-line correction factor can be applied to the ultrasound level detected at the leak source. It is important to be aware that this correction factor can only be used when directly in line with the leak, if this is not possible the inspector should use the highest decibel reading measured by the ultrasonic leak detector at any point around the leak.

6.4 Distance Relationship

The impact on the rate of decay of the ultrasound was investigated to identify whether the 15” distance used by UE Systems when doing an air leak survey is the best option.

As ultrasound has a shorter wavelength than sound in the audible range the attenuation rate is significantly higher, and as was discussed in 3.6.2, due to the divergence of the ultrasonic sound, in combination with factors such as the attenuation, reflection and refraction, the sound level changes as the distance of an ultrasonic leak detector from a leak is altered. This suggests that the level of ultrasound should be measured as close to the leak as will give consistent results.

The effect of either increasing or decreasing the distance to the leak from 15” was studied to show how the level of ultrasound was influenced by varying the distance and to confirm if consistent results could be obtained within the 15” distance currently used.

The ultrasonic sound level was measured at a range of distances from the leak, initially 0.1, 0.15 and 0.3m, to assess the validity of the inverse square law for this application, and to determine if consistent results could be obtained closer to the leak source than the UE Systems standard of between 12” to 15”. Measurements were not taken at the leak site itself to eliminate the possibility of spurious results due to the ultrasonic leak detector interfering with the development of turbulence. As ultrasound generated by compressed air leaks is caused by turbulence created at a leak this could adversely affect any dB readings taken. Further experiments at distances of 0.6, 1.2 and 2.4m were conducted to examine how the ultrasound level reduced over greater distances.

These experiments were conducted to ascertain the consistency and therefore repeatability of any such reduction. The data was then collated and added to the leak characterization chart.

6.4.1 Effect of distance inside 0.3m

An experiment was carried out with a 2.5m length of open ended nylon tubing of 4mm internal diameter at system pressures of 7.01, 4.01, 2.01 and 1.41 Bar_a with respective leak pressures of 2.94, 1.67, 1.15 and 1.08 Bar_a. Measurements were taken at distances of 0.1, 0.15 and 0.3m from the leak to see how the dB level decayed with distance and how the rate of decay was affected at different pressures.

There were three distinct regions in the ultrasonic sound level profiles. These were at, 0°, from 15° to 45° and from 45° to 90°. There were slight variations in these regions caused by geometrical differences between different leaks but they were generally consistent to within a few degrees. Figure 6.9 - Figure 6.12 respectively show the results of these experiments.

The ultrasonic sound levels for each distance were relatively consistent with the profiles at 0.1, 0.15 and 0.3m being very similar. As expected, the sound levels from 0.1m to 0.15m and 0.15m to 0.3m reduced due to the inverse distance law and attenuation. The ultrasonic sound level round the circumference of the leak site was greatly reduced in the centre of the axis of flow. As the distance to the leak in this test was relatively short, it could be as a result of the “cone of silence effect” as discussed by Tam and Auriault. The ultrasonic sound level measured in this cone would be as a result of some of the ultrasound seeping into it. As it is directional, the angle of the cone will increase the distance from the ultrasound wave to the leak detector as long as it is still influenced by the velocity of the flow. This will cause the sound level to reduce more rapidly. As the distance from the leak increases and the influence of the flow reduces, the refraction effect on the ultrasound will subside and mixing will occur.

Table 6.2 shows the dB reduction as the distance from the leak increases. From 0.1m to 0.15m the expected reduction in ultrasound level is 3.5dB when using the inverse distance law, and from 0.15m to 0.3m, it is 6dB. The reduction in ultrasonic sound level from 0.1m to 0.15m at 0° is well above that expected using the inverse distance

law. Looking at the profile of the ultrasonic sound level at 0.1m, it reduced less between 15° to 0° than for either the 0.15m or 0.3m readings in this region. This suggests that the proximity of the detector to the leak the may have led to interference in the developing turbulence, causing higher than expected readings at 0.1m.

The ultrasound reduction in the 15 to 45 region was generally consistent for both 0.1m to 0.15m, and 0.15m to 0.3m and was generally close to the 6dB reduction expected from the inverse distance law, there were one or two anomalies where the dB readings did not match the general trend, these could be caused by fluctuations in the air supply due to loading and unloading of the compressor or errors in the measurement of the ultrasonic sound level, however this would require further investigation for confirmation.

In the region from 45° to 90° the ultrasonic sound level tapered down slowly as the angle relative to the flow direction increased. Again there were fluctuations in this region and further investigation would be required to establish the reasons for this.

The maximum pressure in these tests was 2.94 Bar_a due to the pressure drop through the tubing. Testing at greater distances needed higher pressures to confirm if the sound level reduction over distance remained constant.

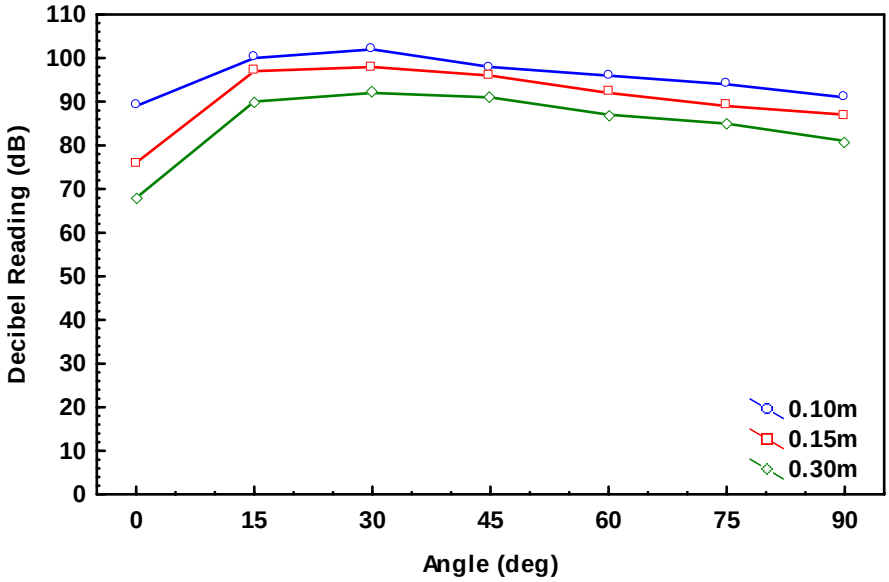

Figure 6.9, dB Readings taken at a distance of 0.10, 0.15 and 0.30m from a round leak source of 4mm diameter. Pressure at leak 2.94 Bar_a.

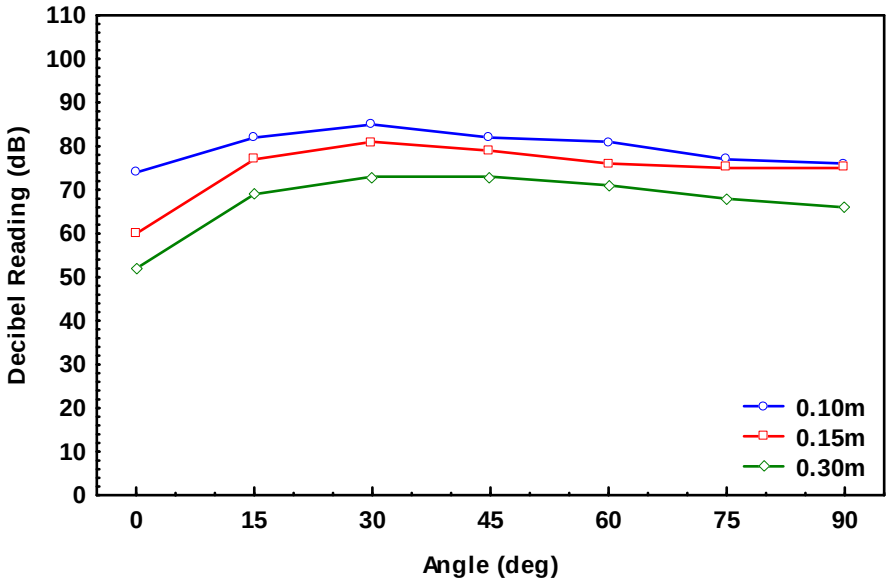

Figure 6.10, dB readings taken at a distance of 0.10, 0.15 and 0.30m from a round leak source of diameter 4mm. Pressure at leak 1.67 Bar_a.

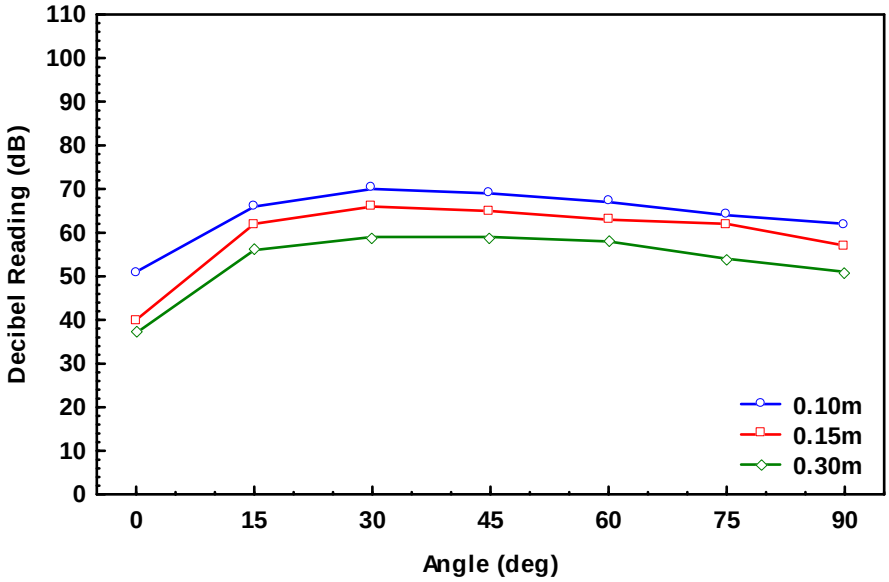

Figure 6.11, dB readings taken at a distance of 0.10, 0.15 and 0.30m from a round leak source of 4mm diameter. Pressure at leak 1.15 Bar_a.

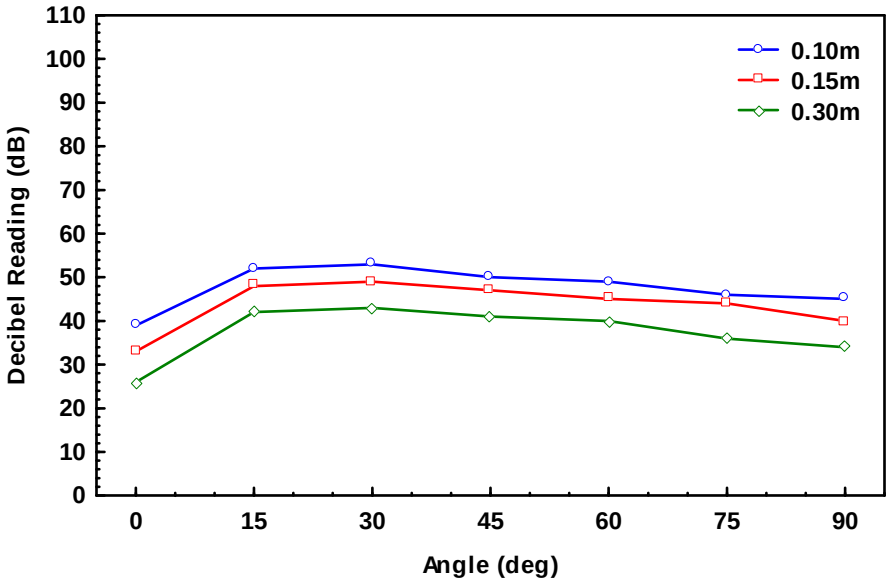

Figure 6.12, dB reading taken at a distance of 0.10, 0.15 and 0.30m from a round leak source of 4mm diameter, pressure at leak 1.08 Bar_a.

Figure 6.13 shows how the previous results translated when the maximum sound level for each leak was plotted against the distance from the leak. Using a logarithmic scale allows a true comparison of the rate of decay of the ultrasound signal. The rate of decay is consistent at each of the four pressures tested, which shows that the ultrasound decays at the same rate for different leak pressures. The decay of the

ultrasound from 0.1m to 0.15m and from 0.15m to 0.3m was plotted and shows that the rate of decay for the maximum ultrasound signal at both distances was the same. This is a significant finding as it implies that the level of ultrasound could be measured at 0.1m from the leak as there is consistency between the different pressures.

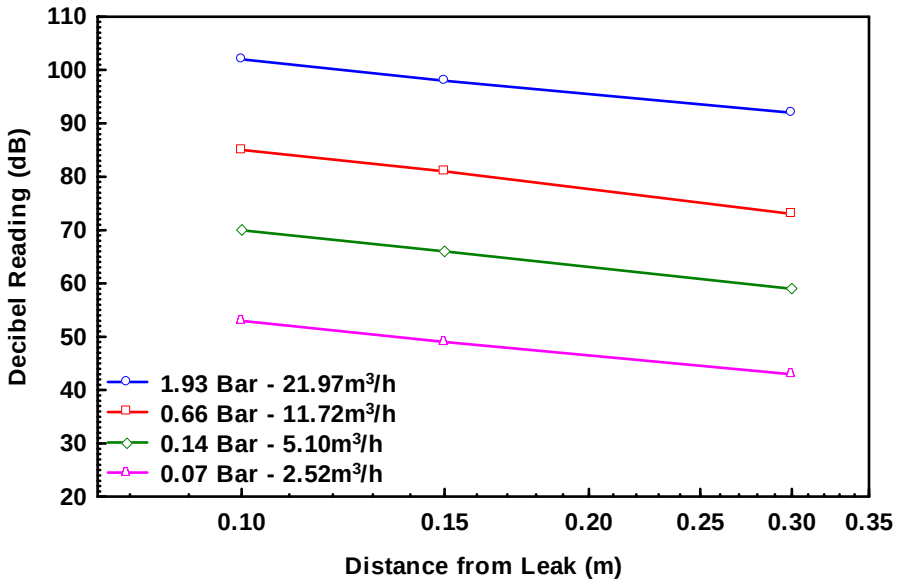

Figure 6.13, Rate of decay of ultrasonic sound level with increasing distance from an open ended tube of length 2.5m and diameter 4mm (nom.), for a range of pressures.

Table 6.2, dB reduction between 0.1 - 0.15mm, (3.5dB reduction expected using Inverse Distance Law), and 0.15 - 0.3mm, (6dB expected using Inverse Distance Law), from 0-90° for leak pressures of 2.94, 1.67, 1.15 and 1.08 Bar_a.

	Angle	0°	15°	30°	45°	60°	75°	90°
Dist. to Leak	Exit Press.	dB Drop (+/-1dB)						
0.1 - 0.15m	1.93Bar	13	3	4	2	4	5	4
	0.66Bar	14	5	4	3	5	2	1
	0.14Bar	11	4	4	4	4	2	5
	0.07Bar	6	4	4	3	4	2	5
0.15 - 0.3m	1.93Bar	8	7	6	5	5	4	6
	0.66Bar	8	8	8	6	5	7	9
	0.14Bar	3	6	7	6	5	8	6
	0.07Bar	7	6	6	6	5	8	6

6.4.2 Effect of Distance beyond 0.3m

To ascertain if the inverse distance law could still be used at greater distances, tests using orifice plates of two leak geometries were carried out. One had a 1.6mm diameter round hole and the other a 1mm x 15mm slot. The tests used nominal pressures of 1.41, 2.01, 4.01 and 7.01* Bar_a, (* 6.31 Bar for 1mm x 15mm slot as system was unable to reach 7.01 Bar_a). Measurements of the ultrasonic sound level were taken at 0.6, 1.2 and 2.4m from the leak site and at 15° intervals between 0° and 45°. As space in the laboratory was limited it was not possible to measure the ultrasonic sound level beyond a 45° angle, however, as the previous experiments had shown that dB peaked between 30° and 45° for a round jet this was not crucial in terms of this study.

In this series of tests there are two distinct regions, there is the region at 0°, and the region from 15° to 45°. Once again there are significant variations between results in the axis of the flow (0°) while the results for the 15° to 45° region can be seen to be more consistent. The results are shown in Figure 6.14 - Figure 6.17.

As was seen in 6.4.1, the lowest ultrasonic sound level was found at 0°, while the peak level was at approximately 30° for the reasons described, this profile was maintained in the tests performed at distances greater than 0.3m, however, the levels of the variation in the ultrasound were significantly different at greater distances.

Table 6.3 shows the ultrasonic sound level reduction from 0.6m to 1.2m and from 1.2m to 2.4m for each angle and pressure. The expected reduction when using the inverse distance law would be 6dB for both distances in this study. At 0° the reduction in ultrasonic sound level varied significantly between tests, the ultrasound level from 15° to 0° at 1.2m reduced significantly less than at other distances and was higher than at 0.6m in several cases. The reason for this could not be ascertained as it did not follow the expected theory, and after examining the data used in the tests there was no obvious cause. As the sound level in this region is not crucial in the

development of the leak characterization chart no further investigation was undertaken at this time.

At 0° between the distances of 1.2m and 2.4m, a reduction of more than 21dB was measured in all cases. The results indicated that the reduced ultrasonic sound level along the flow axis was caused by the faster flowing air in the core of the jet refracting the slower moving air at the shear layer. This in combination with the attenuation that was occurring in the 15° to 45° region as the distance from the leak source increased, meant that the level of ultrasound reaching the central core at 2.4m from this region would have lessened, hence the ultrasonic sound level would reduce more rapidly in the jet core.

In the region from 15° to 45° the profiles of the sound levels correspond to each other more closely, although there is a degree of variation in the results

The data shows that, in this region, from 0.6m – 1.2m the dB drop was still relatively consistent with the inverse square rule for both leak geometries, but with slightly more variation than at shorter distance. However between 1.2 and 2.4m the reduction in the ultrasonic sound level has increased considerably, due to attenuation of the short wavelength ultrasound.

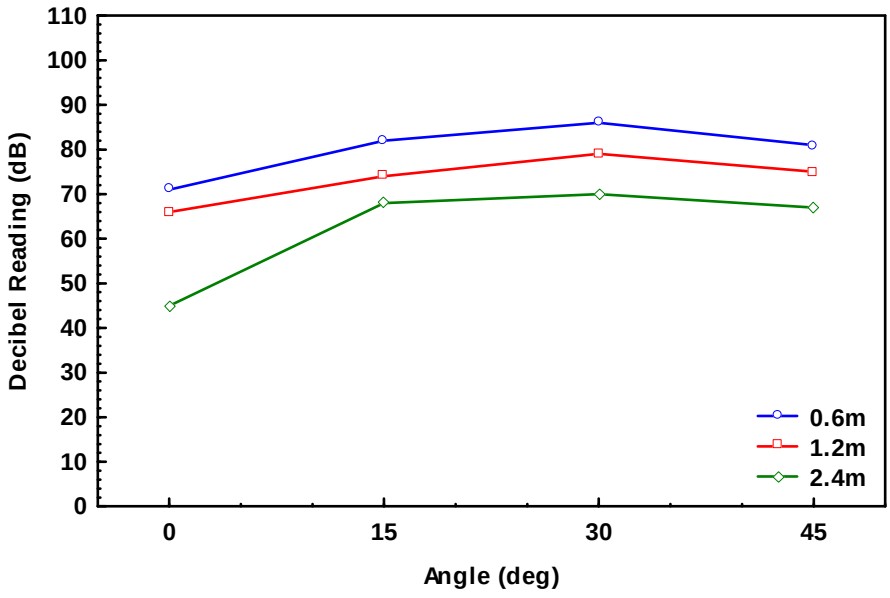

Figure 6.14, dB Reading taken at a distance of 0.6, 1.2 & 2.4m from a round leak source of diameter 1.6mm at a line pressure of 7.01 Bar_a.

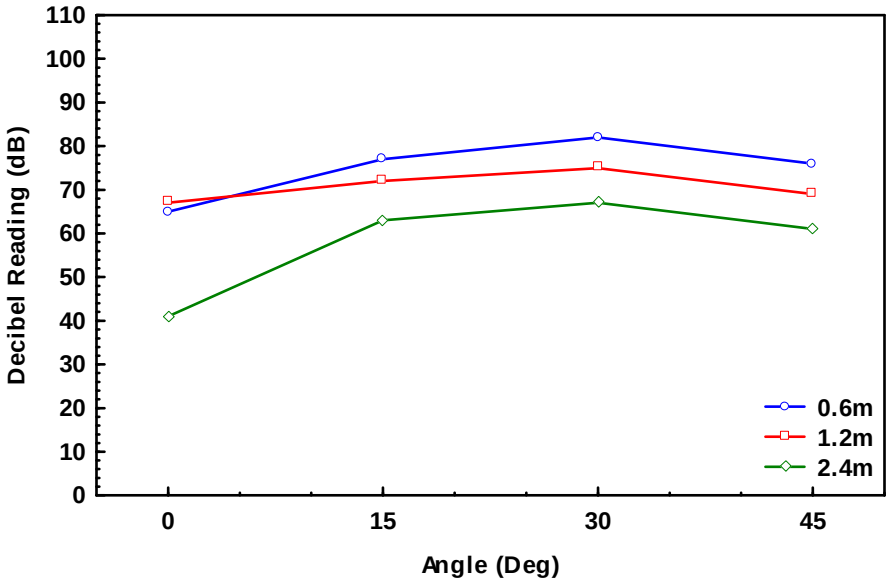

Figure 6.15, dB Reading taken at a distance of 0.6, 1.2 & 2.4m from a round leak source of diameter 1.6mm at a line pressure of 4.01 Bar_a.

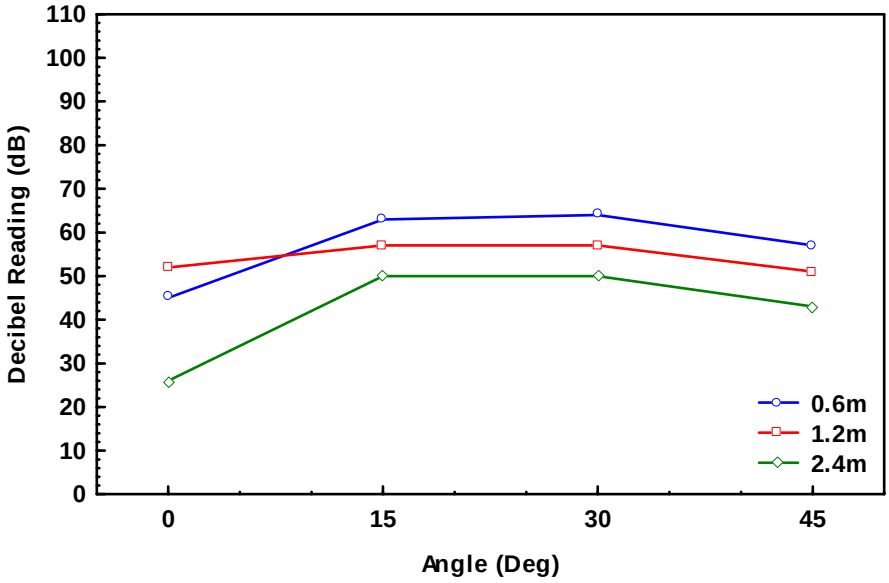

Figure 6.16, dB Reading taken at a distance of 0.6, 1.2 & 2.4m from a round leak source of diameter 1.6mm at a line pressure of 2.01 Bar_a.

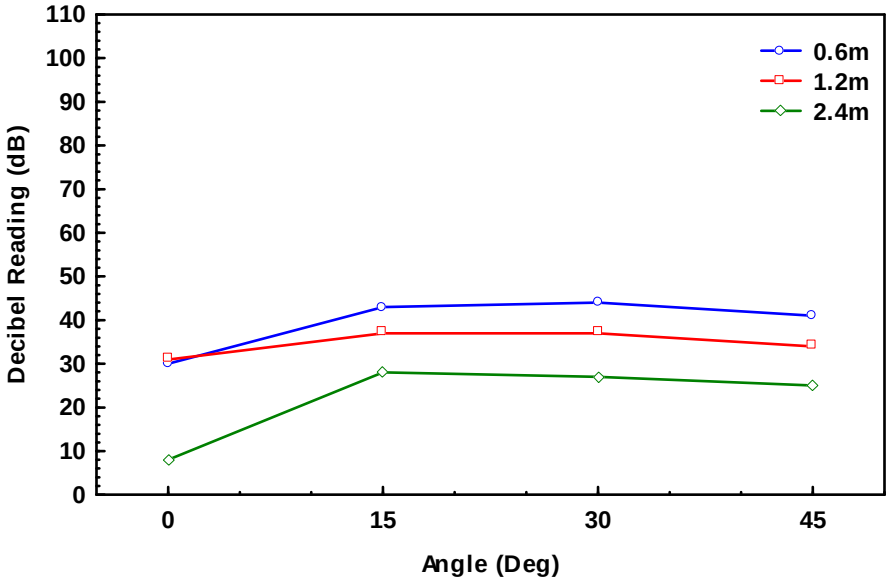

Figure 6.17, dB Reading taken at a distance of 0.6, 1.2 & 2.4m from a round leak source of diameter 1.6mm at a line pressure of 1.41 Bar_a.

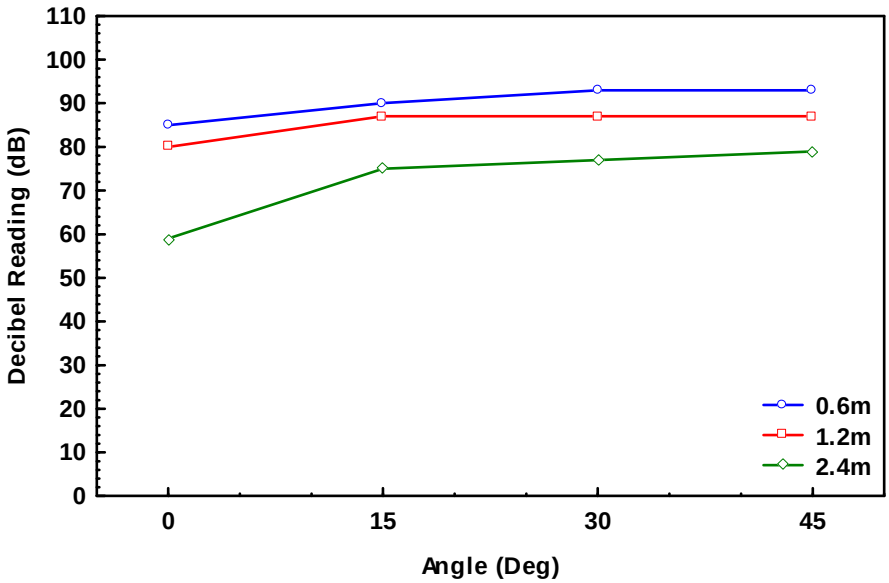

Figure 6.18, dB Reading taken at a distance of 0.6, 1.2 & 2.4m from a rectangular leak of dimensions 1mm x 15mm at a line pressure of 6.31 Bar_a.

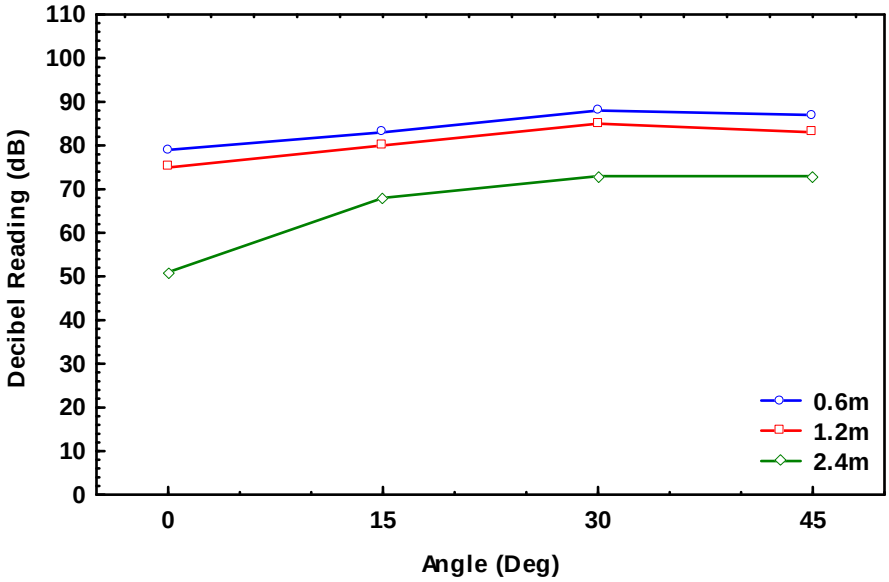

Figure 6.19, dB Reading taken at 0.6, 1.2 & 2.4m from a rectangular leak source of 1mm x 15mm at a line pressure of 4.01 Bar_a.

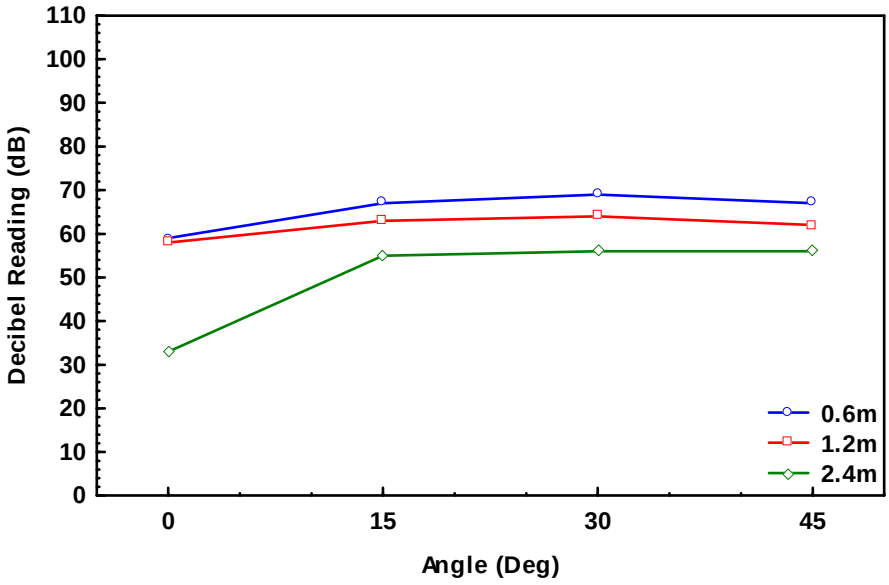

Figure 6.20, dB Reading taken at 0.6, 1.2 & 2.4m from a rectangular leak source of 1mm x 15mm at a line pressure of 2.01 Bar_a.

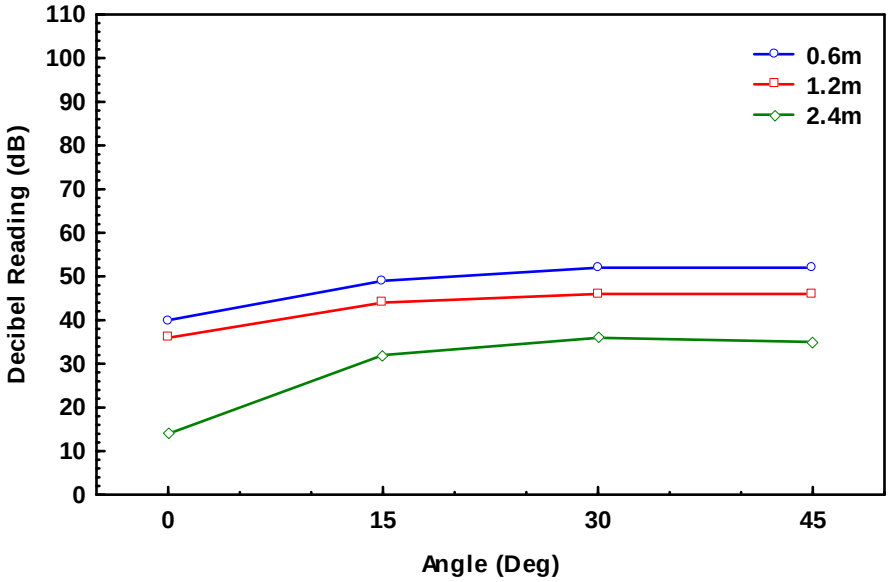

Figure 6.21, dB Reading taken at 0.6, 1.2 & 2.4m from a rectangular leak source of 1mm x 15mm at a line pressure of 1.41 Bar_a.

As with the results for the ultrasound level reduction from 0.1m to 0.3m the results in Figure 6.22Figure 6.23 have been plotted on a logarithmic scale. The fluctuations in the rate of the ultrasound level reduction from 0.6m to 1.2m, and, 1.2m to 2.4m for the different leak pressures, shows that the level of ultrasound is less consistent at greater distances, which is most probably as a result of attenuation or reverberation.

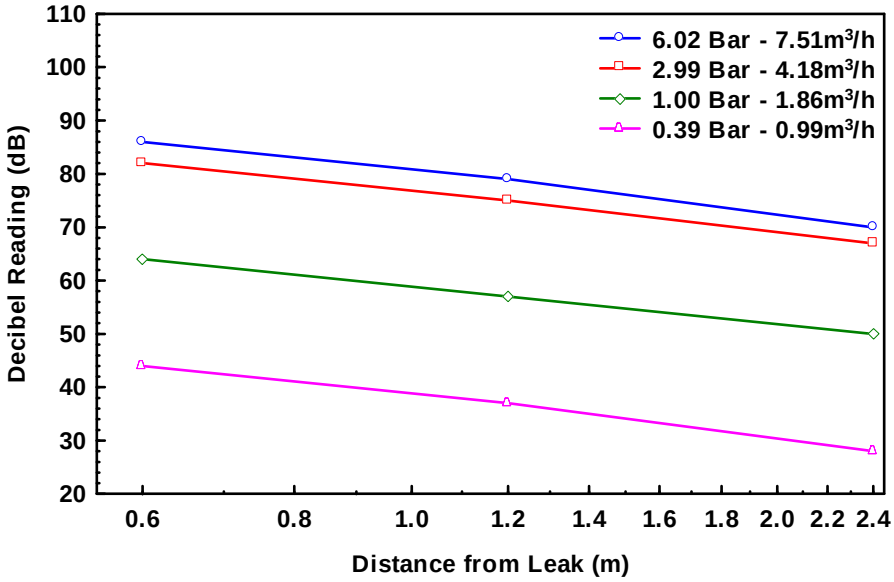

Figure 6.22 Rate of decay of ultrasonic sound level with increasing distance from a round hole of diameter 1.6mm (nom.), for a range of pressures.

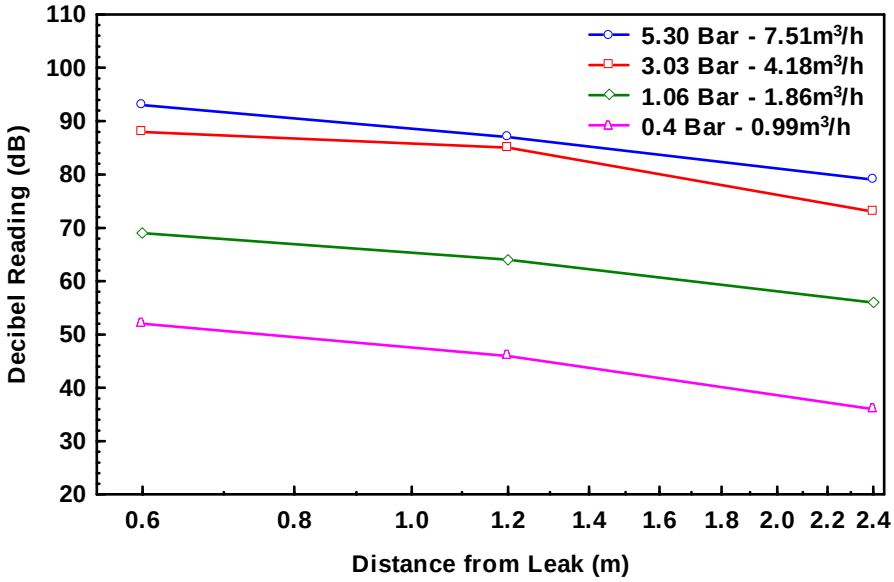

Figure 6.23 Rate of decay of ultrasonic sound level with increasing distance from a rectangular slot of dimensions 1mm x 15mm(nom.), for a range of pressures.

Table 6.3, dB drop between 0.6m to 1.2m, and 1.2m to 2.4m from 0° - 45° for a 1.6mm diameter hole at 7.03, 4.00, 2.01 & 1.4 Bar_a and a 1mm x 15mm slot at 6.31, 4.04, 2.07 & 1.41 Bar_a. (6dB reduction expected using Inverse Distance Law for both distances).

		Angle	0°	15°	30°	45°
Leak Type	Dist. To Leak	Exit Press.	dB Drop (+/-1dB)			
1.6mm Diameter Hole	0.6 - 1.2m	7.03 Bar	5	8	7	6
		4.00 Bar	-2	5	7	7
		2.01 Bar	-7	6	7	6
		1.40 Bar	-1	6	7	7
	1.2m - 2.4m	7.03 Bar	21	6	9	8
		4.00 Bar	26	9	8	8
		2.01 Bar	26	7	7	8
		1.40 Bar	23	9	10	9
1mmx15mm Slot	0.6 - 1.2m	6.31 Bar	5	3	6	6
		4.04 Bar	4	3	3	4
		2.07 Bar	1	4	5	5
		1.41 Bar	4	5	6	6
	1.2m - 2.4m	6.31 Bar	21	12	10	8
		4.04 Bar	24	12	12	10
		2.07 Bar	25	8	8	6
		1.41 Bar	22	12	10	11

6.4.3 Summary

When carrying out a compressed air leak survey or audit it is important that the data being collected is accurate. This tests in this section showed how over a relatively short distance the variations in ultrasonic sound level change considerably.

Competing ultrasounds can be a considerable influence on ultrasonic sound levels being measured from a leak. As the risk increases with distance, it is important that any measurements are taken as close as possible to a leak.

A consistent ultrasonic sound level reduction was attained between 0.10m (100mm) and 0.15m (150mm) when taking the maximum decibel level, however there was considerable variation over the full range of measurement angles at 0.1m distance from the leak. The levels of ultrasound were most consistent at 0.15m and 0.3m from the leak, to ensure predictability of results at the shortest distance to the leak a distance of 0.15m is recommended. This is half the distance from a leak of the current operating standard used for the UE Systems “Guess-timator” chart. Using this distance as the standard will help to reduce potential errors due to external influences such as competing ultrasounds. Beyond the current operating distance of between 0.3m and 0.4m there was increased fluctuation in the measured ultrasound and therefore any measurements beyond this should be treated with caution.

6.5 Length Effect

The length of air line prior to a leak was tested to determine the influence of this on the flow rate of the air escaping at a leak site.

To examine the impact on the leak pressure of increasing the length of the tubing, 1.0, 2.5, 5.0, 7.5, 10 & 25m lengths of nylon tubing were tested at line pressures of 0.4, 0.6, 1.0, 3.0 and 6.0 Bar (all gauge) to examine how the pressure and hence volume flow rate of the air in the tubing reduced for each length. The tests were carried out

for three diameters of tubing, 2.5, 4.0, 6.0mm to determine whether this had any effect on the rate of decay.

The line pressure was measured in advance of the manifold to which the tubing was attached, and the leak pressure was measured using a pressure transducer 30mm prior to the exit of the tubing. The results are displayed as a ratio of leak pressure to supply pressure for a given length. The ratio of p_L to p_S was calculated at gauge pressure, as the curve tends to a least asymptote of zero. If absolute pressure was used then the Leak pressure would never reduce below 1.01 Bar_a and the pressure ratio would never reach zero.

Figure 6.24 -Figure 6.28 show that for all supply pressures, a considerable pressure reduction occurred even through a 1m length of tubing. As the length of tubing was increased further, this reduction in pressure slowed and although the overall pressure drop was greater the increase in length had a diminishing effect.

Comparing the pressure drop ratio at high and low pressures, the ratio was similar in all cases for a 1m length of tubing. At higher pressures, (e.g. 6 Bar_g), as the length increased and the leak pressure reduced, there was a large pressure differential and the ratio became very small. At lower pressures (e.g. 0.4 Bar_g), this pressure differential was much smaller as the leak pressure stabilised at 0.1 Bar_g and hence the pressure drop ratio was much larger. Although this leak pressure may reduce further with increased length, the rate is so slight that it can be ignored.

In Figure 6.27 and Figure 6.28, where the supply pressures are 0.6 Bar_g and 0.4 Bar_g respectively, there pronounced fluctuations in the profile of the pressure decay, this may have been due to the supply pressures being time averaged over the duration of the experiment, at such low pressures any minor fluctuation appeared considerable, whereas in reality they were only 0.01 Bar_g – 0.02 Bar_g.

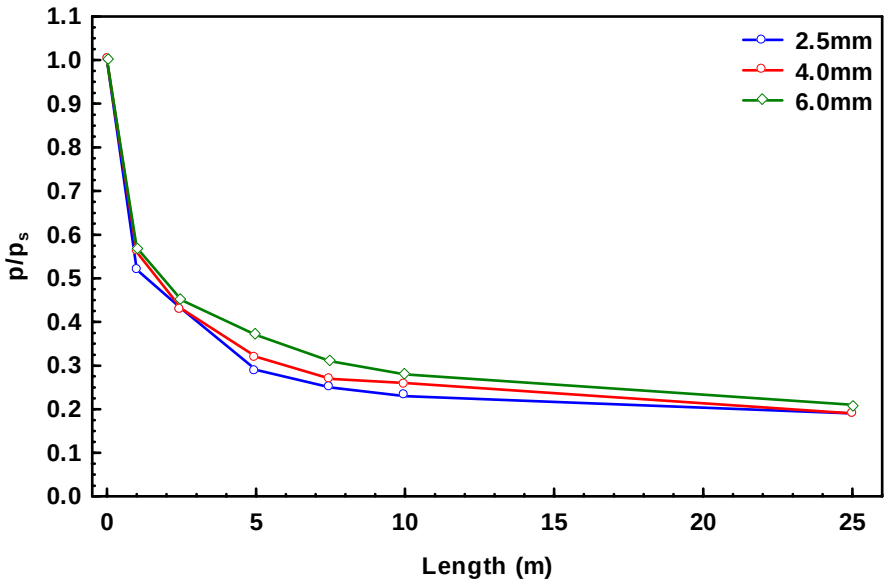

Figure 6.24, Profile of pressure drop ratio, for tubing of lengths 1, 2.5, 5, 7.5, 10 and 25m and diameters 2.5, 4.0, 6.0mm at a supply pressure of 6 Bar_g.

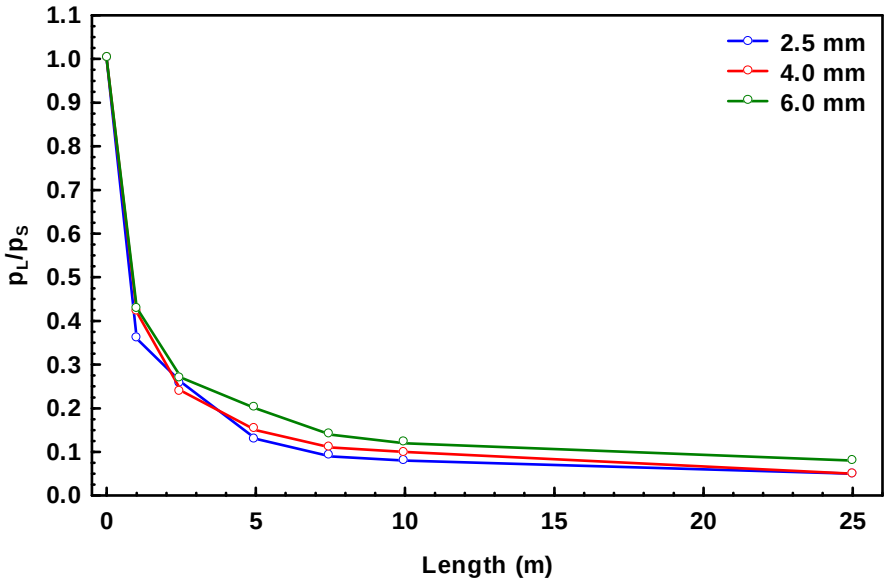

Figure 6.25, Profile of pressure drop ratio, for tubing of lengths 1, 2.5, 5, 7.5, 10 and 25m and diameters 2.5, 4.0, 6.0mm at a supply pressure of 3 Bar_g.

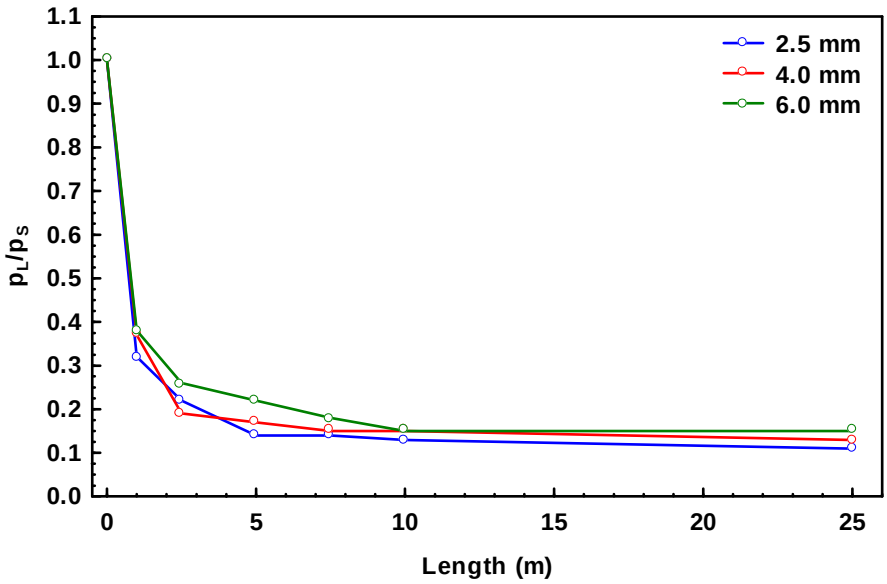

Figure 6.26, Profile of pressure drop ratio, for tubing of lengths 1, 2.5, 5, 7.5, 10 and 25m and diameters 2.5, 4.0, 6.0mm at a supply pressure of 1 Bar_g.

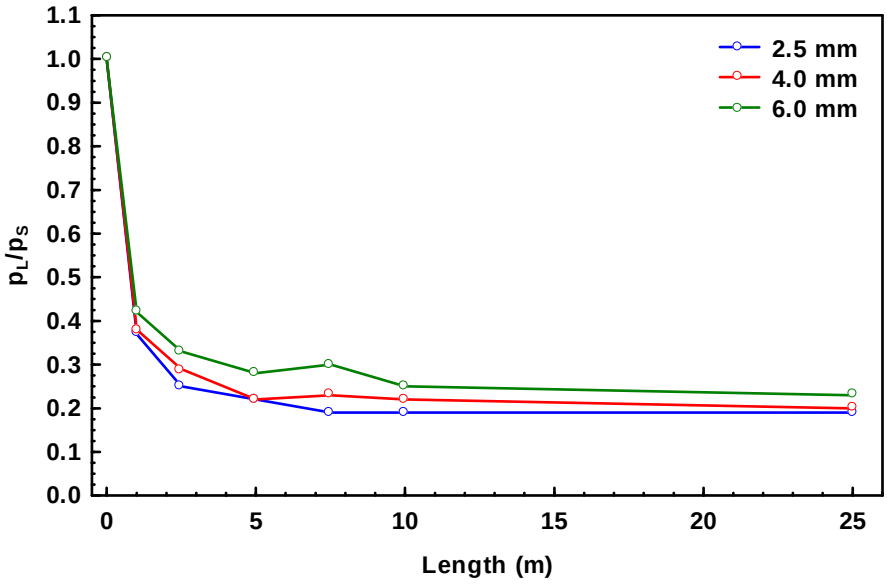

Figure 6.27, Profile of pressure drop ratio, for tubing of lengths 1, 2.5, 5, 7.5, 10 and 25m and diameters 2.5, 4.0, 6.0mm at a supply pressure of 0.6 Bar_g.

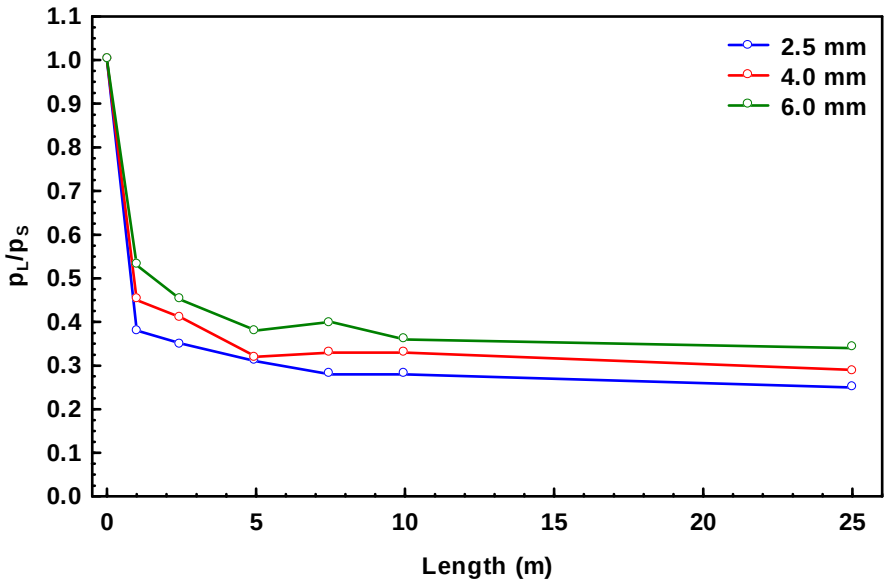

Figure 6.28, Profile of pressure drop ratio, for tubing of lengths 1, 2.5, 5, 7.5, 10 and 25m and diameters 2.5, 4.0, 6.0mm at a supply pressure of 0.4 Bar_g.

Table 6.4, Ratios of leak pressure to supply pressure for tubing of diameters 2.5, 4.0 and 6.0mm, and at lengths of 1.0, 2.5, 5.0, 7.5, 10, and 25m at supply pressures of 0.4, 0.6, 1.0, 3.0 and 6.0 Bar_g.

		Pressure Drop Ratio (p_L / p_S)				
	Length (m)	6bar	3bar	1bar	0.6bar	0.4bar
2.5mm Diameter	1.0	0.45	0.36	0.32	0.37	0.38
	2.5	0.33	0.25	0.22	0.25	0.35
	5.0	0.18	0.13	0.14	0.22	0.30
	7.5	0.12	0.09	0.14	0.18	0.28
	10.0	0.10	0.08	0.13	0.18	0.28
	25.0	0.05	0.05	0.11	0.18	0.25
4.0mm Diameter	1.0	0.49	0.42	0.32	0.37	0.38
	2.5	0.33	0.24	0.22	0.25	0.35
	5.0	0.21	0.15	0.14	0.23	0.30
	7.5	0.15	0.11	0.14	0.18	0.28
	10.0	0.14	0.10	0.13	0.18	0.28
	25.0	0.06	0.05	0.11	0.18	0.25
6.0mm Diameter	1.0	0.49	0.43	0.38	0.42	0.53
	2.5	0.37	0.27	0.26	0.33	0.45
	5.0	0.27	0.20	0.22	0.28	0.38
	7.5	0.19	0.14	0.18	0.30	0.40
	10.0	0.17	0.12	0.15	0.25	0.35
	25.0	0.08	0.08	0.15	0.23	0.35

A summary of the pressure drop ratios is given in Table 6.4, as only the 6 Bar_g and 3 Bar_g supply pressures are relevant for the majority of industrial compressed air systems these columns have been highlighted for clarity.

Although there are variations in the pressure drop ratios for the various pipe diameters, when being applied to an air leak in an industrial plant they are within an acceptable range to still offer a significant improvement to the accuracy of any estimation of leak rate. At 6 Bar_g a correction factor of 0.49 at 1m or 0.22 at 5m could quite safely be applied to the flow rate for a given orifice size that is quoted in the "Discharge of Air Through an Orifice" table included in the UE Systems "Compressed Air Guide". While mentioning this table, it is also worth highlighting a

common error made when obtaining a flow rate from it. When quoting the line diameter to obtain a flow rate, it is imperative that it is the inside diameter that is used and not the outside diameter. For example, in the table the difference between quoting a 1/4" line as opposed to a 1/8" is approximately 71cfm(120m^3/h) at 90psig (6.2 Bar_g), even if it is a 1m line and a correction factor of 0.5 is applied, this still equates to an over estimation in the flow rate of about 35cfm (60m^3/h).

6.6 Leak Shape

Orifices of different shapes and sizes were set up to represent a variety of leaks in a compressed air distribution network. As Compressed air leaks come in many guises, the relationship between cross sectional area, aspect ratio and diameter were investigated to identify any obvious trends between the ultrasound level from a leak and the geometry of the orifice. If obvious trends were identified correction factors could be developed and included in the leak characterisation chart.

A coefficient of discharge was calculated for each of the different leaks at a number of pressures to identify whether this varied with leak geometry and if this was the case to include it in the leak characterisation chart to take account of non ideal effects at a leak source.

Sections 6.6.1 and 6.6.2 investigate whether variations in geometry affect the leak rate from orifices of a constant area. The results were analysed and the following graphs plotted for each of the test pieces in both groups of tests.

1) Volumetric flow rate against pressure at the leak for the actual cross sectional area
2) Area corrected, volumetric flow rate against pressure at the leak.
3) Ultrasonic Sound Level (dB) against Pressure.
4) Ultrasonic Sound Level(dB) against Volumetric Flow Rate.

6.6.1 Aspect Ratio Comparison

To ascertain if aspect ratio affected the flow rate and associated ultrasonic sound level from a specific size of leak the previously stated orifice plates were tested at set supply pressures of 1.41, 2.01, 4.01 and 7.01 Bar. If there are obvious variations in the flow rate or ultrasonic sound level for leaks with the same cross sectional area but different aspect ratio, it may allow a correction factor to be developed to take account of these when conducting a leak survey.

A number of orifice plates were manufactured with a common cross sectional area but different aspect ratios to enable flow rates and ultrasonic sound levels for these conditions to be compared. As was discussed in 5.1.2, there were minor differences in the cross sectional areas of the test pieces due to the tolerances inherent in the manufacturing process. This was visible in the results of the tests, as small variations in the geometries made a high level of accuracy very difficult. There were three groups set up for aspect ratio comparison with a minimum of two test pieces for comparison. These groups were as follows (corrected dimensions in brackets):

Aspect Ratio Comparison

1) 5mm^2	1mm x 5mm Slot……..(5.47mm^2)
	0.5mm x 10mm Slot…….(6.05mm^2)
2) 7.5mm^2	0.75mm x 10mm Slot……...(7.69mm^2)
	0.5mm x 15mm Slot…….(9.37mm^2)
3) 15mm^2	0.5mm x 30mm Slot…….(18.75mm^2)
	0.75mm x 20mm Slot……...(15.75mm^2)
	1mm x 15mm Slot……(15.08mm^2)
	2mm x 7.5mm Slot……...(14.92mm^2)

The volumetric flow rates in Figure 6.29Figure 6.31 give the actual measured flow through each of the orifices. To allow the aspect ratios of the test pieces to be

compared the volumetric flow rates were corrected for area to take account of the variation in sizes.

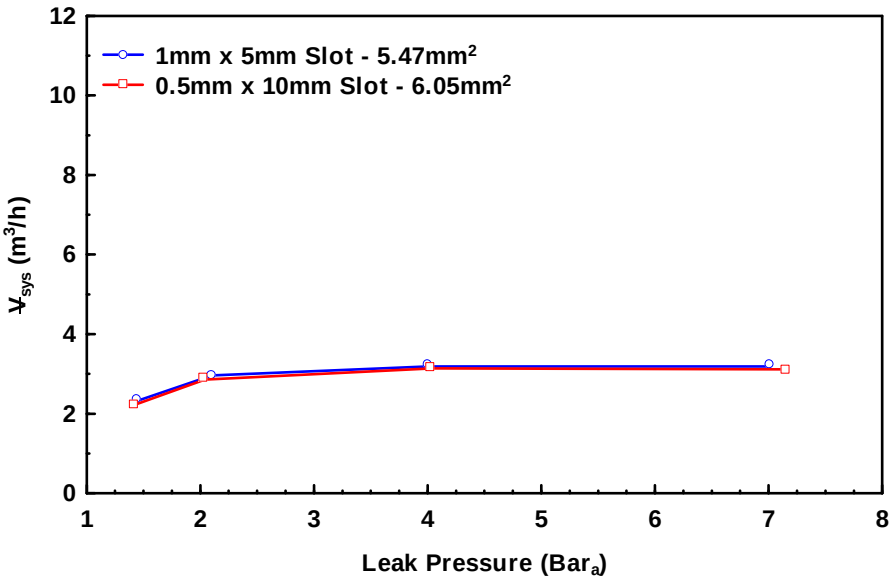

Figure 6.29, Volumetric flow rate comparison of two orifices with cross sectional areas of 5.47mm^2 and 6.05mm^2 at line pressures of 1.41, 2.01, 4.01, 7.01 Bar$_a$, nominal.

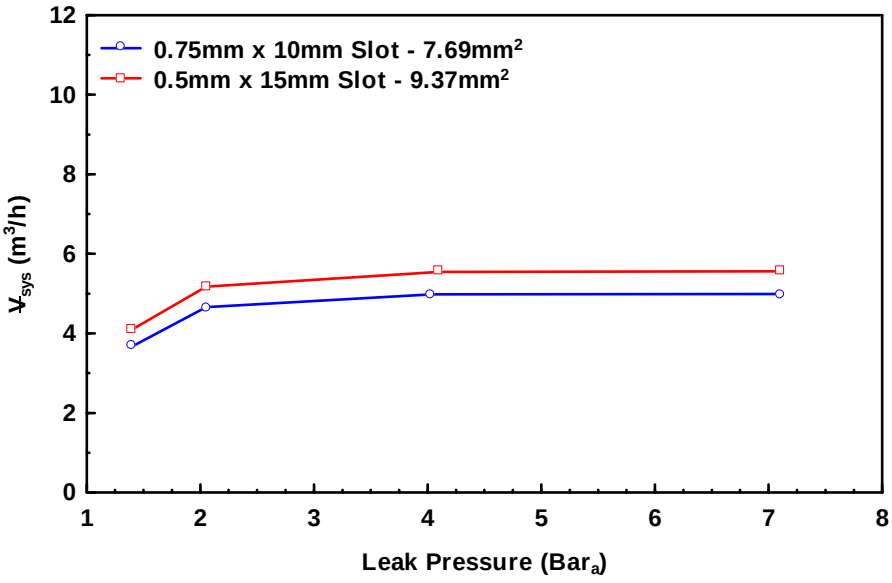

Figure 6.30, Volumetric flow rate comparison of two orifices with cross sectional areas of 7.69mm^2 and 9.37mm^2 at line pressures of 1.41, 2.01, 4.01, 7.01 Bar$_a$, nominal.

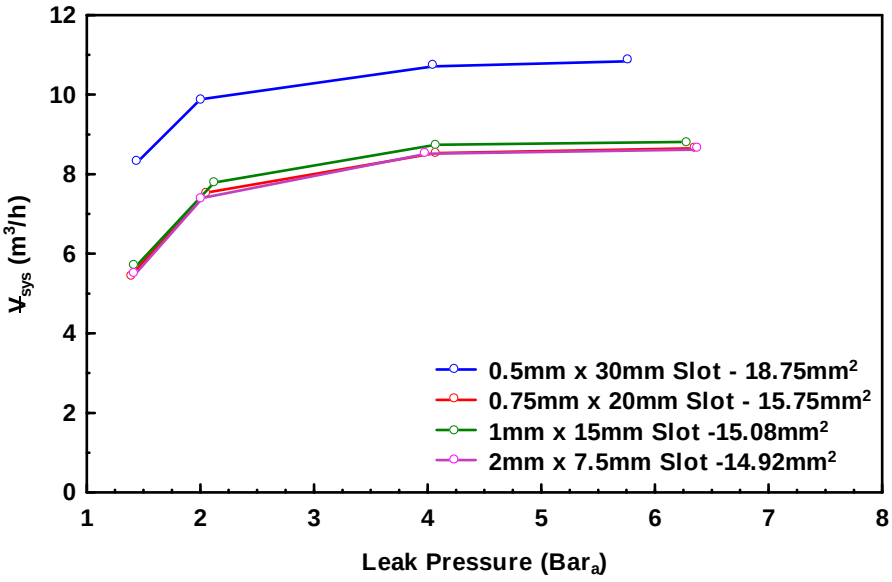

Figure 6.31, Volumetric flow rate comparison of two orifices with cross sectional areas of 18.75mm^2, 15.75mm^2, 15.08mm^2 and 14.92mm^2 at line pressures of 1.41, 2.01, 4.01, 7.01 Bar$_a$, nominal.

Figure 6.32 -Figure 6.34 show the volumetric flow rates corrected for area plotted against the leak pressure. While the dimensions used for theses plots are considerably more accurate than those used in Figure 6.29 Figure 6.31, they are still not completely accurate as was discussed in 5.1.2. The variation in the volumetric flow rates for the different aspect ratios is minor in all three tests, to be entirely confident in the results more accurately prepared and dimensioned test pieces would be required.

Any variation in volumetric flow rate for leaks of constant area but different aspect ratios can be seen to be minimal. As there are no significant variations, aspect ratio can be ignored as a factor when developing the leak characterisation chart.

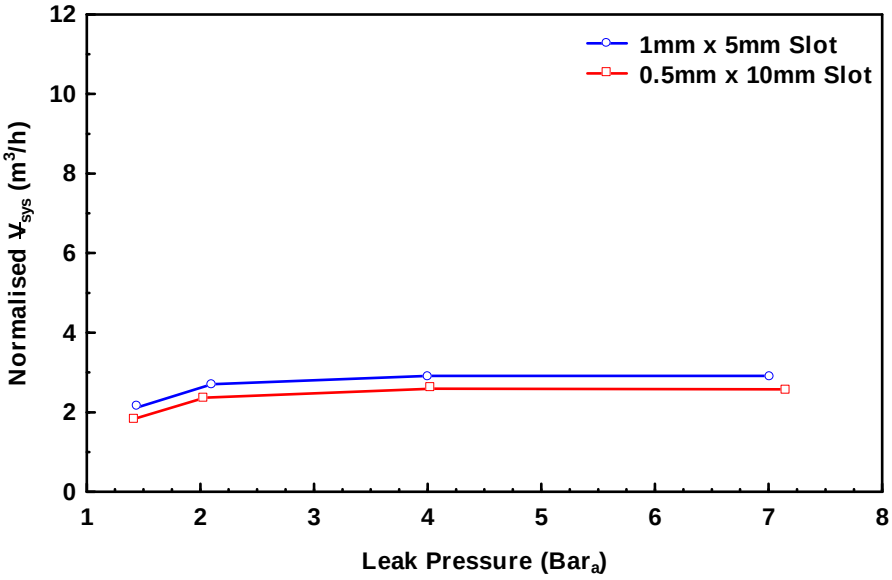

Figure 6.32, Volumetric flow rate normalised to a cross sectional area of 5mm^2 at line pressures of 1.41, 2.01, 4.01, 7.01 Bar_a, nominal.

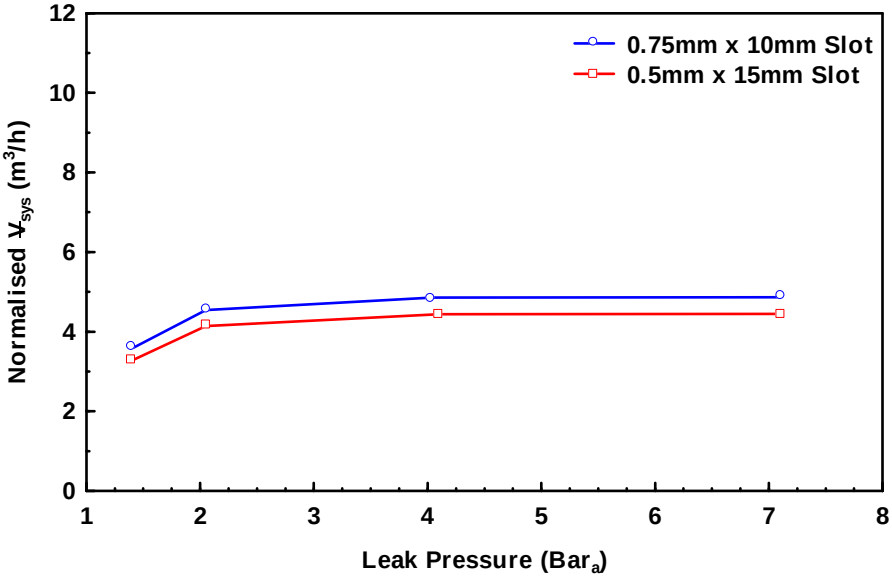

Figure 6.33, Volumetric flow rate normalised to a cross sectional area of 7.5mm^2 at line pressures of 1.41, 2.01, 4.01, 7.01 Bar_a, nominal.

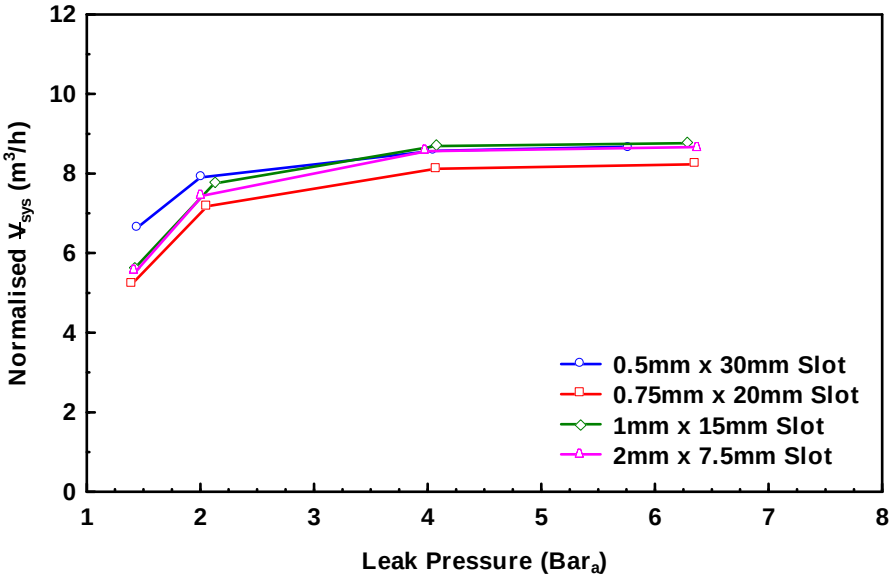

Figure 6.34, Volumetric flow rate normalised to a cross sectional area of 15mm^2 at line pressures of 1.41, 2.01, 4.01, 7.01 Bar$_a$, nominal.

The ultrasonic sound level was measured for each of the tests in the above section to ascertain if the sound generated at the leak was affected by variations in aspect ratio. As in previous tests, the ultrasound was measured in an arc around the leak site at a distance of 0.3m. The highest level of ultrasound recorded for each leak was used for each test. Figure 6.35Figure 6.37 are plots of the maximum ultrasonic sound level against pressure. When these were compared to the plots of the area corrected flow rates it showed that the lower ultrasonic sound levels correspond to the lower flow rates.

While these results could be revisited through the testing of more accurate test pieces to confirm the relationship between the ultrasound level and the aspect ratio, the results indicate that as with the flow rates, any variation in the ultrasound level due to aspect ratio is minimal and will be ignored in the development of the leak characterisation chart.

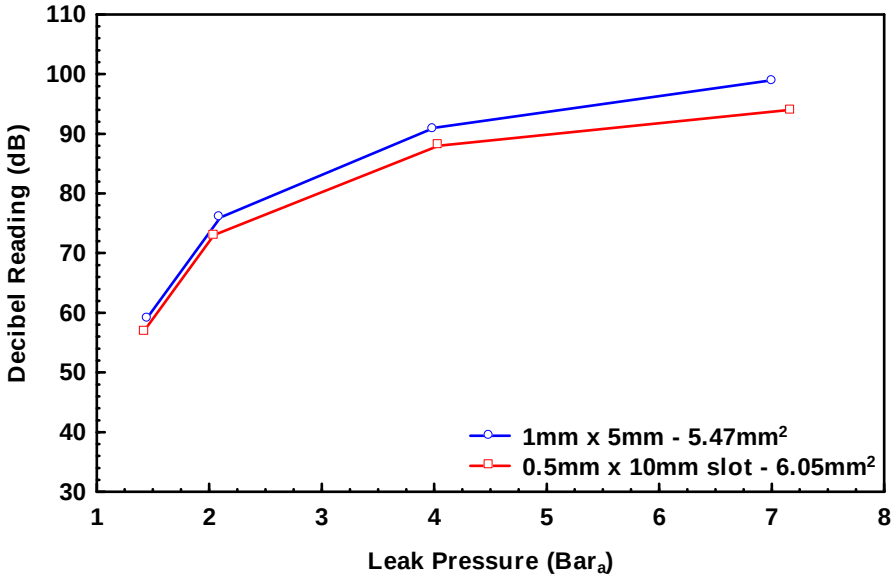

Figure 6.35, Ultrasonic sound level at 0.3m from source for orifices of 5.47mm^2 and 6.05mm^2 at line pressures of 1.41, 2.01, 4.01, 7.01 Bar$_a$, nominal.

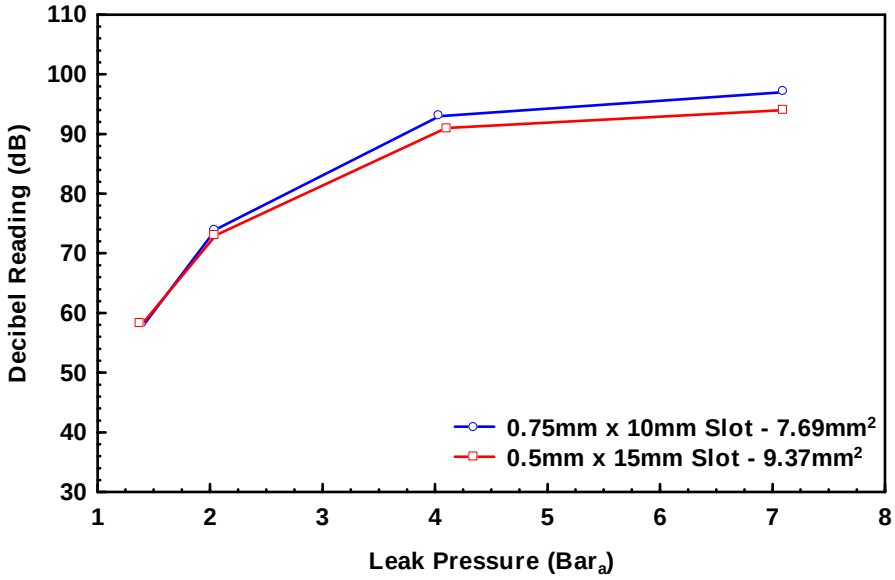

Figure 6.36, Ultrasonic sound level at 0.3m from source for orifices of 7.69mm^2 and 9.37mm^2 at line pressure of 1.41, 2.01, 4.01, 7.01 Bar$_a$, nominal.

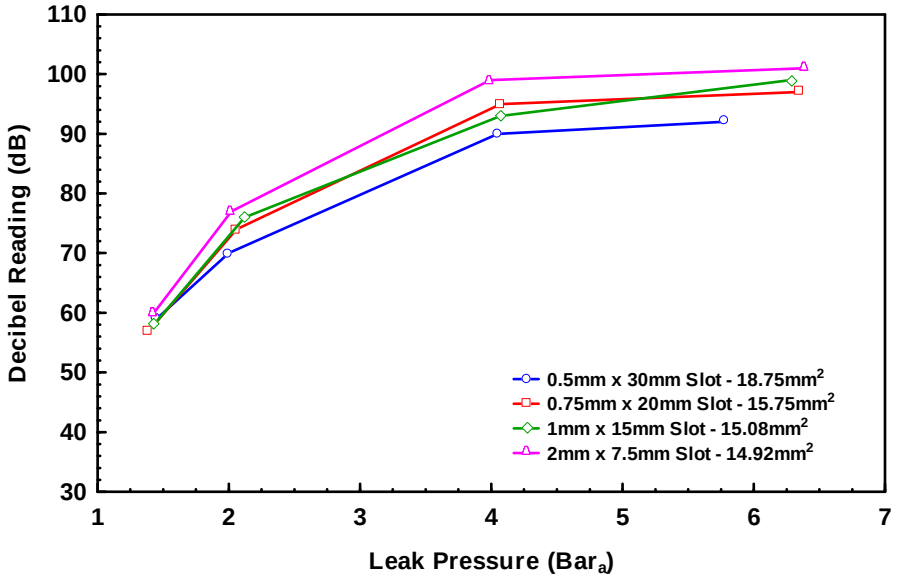

Figure 6.37, Ultrasonic sound level at 0.3m from source, for orifices of 18.75mm^2, 15.75mm^2, 15.08mm^2 and 14.92mm^2 at line pressures of 1.41, 2.01, 4.01, 7.01 Bar$_a$, nominal.

The ultrasonic sound level measured at 0.3m from the leak site was plotted against the volumetric flow rate of the air in the system as shown in Figure 6.38Figure 6.40. Using these graphs, for a known leak size and a measured decibel reading, the actual volumetric flow rate can be calculated by correcting for pressure.

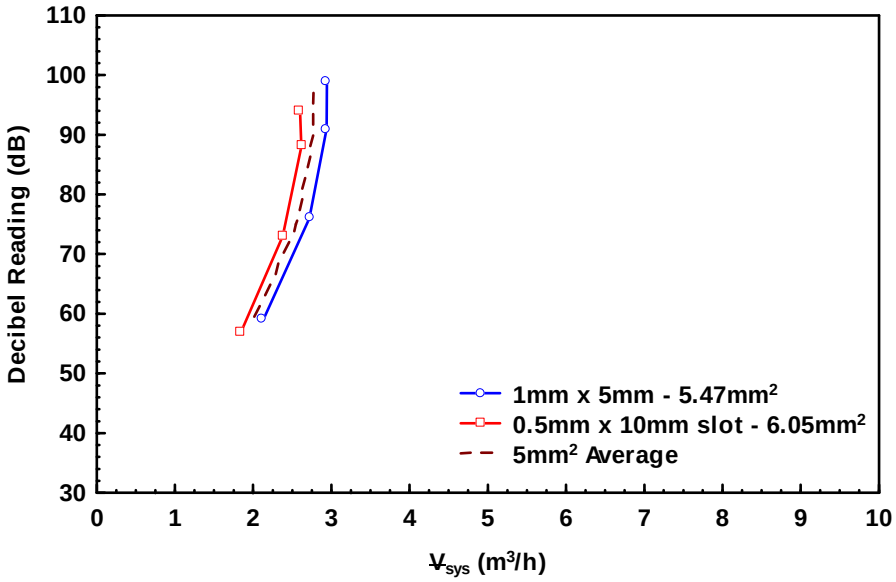

Figure 6.38, Ultrasonic sound level at 0.3m from source plotted against the uncorrected volumetric flow rate for orifices of 5.47mm^2 and 6.05mm^2, at leak pressures of 1.41, 2.01, 4.01, 7.01 Bar$_a$, nominal.

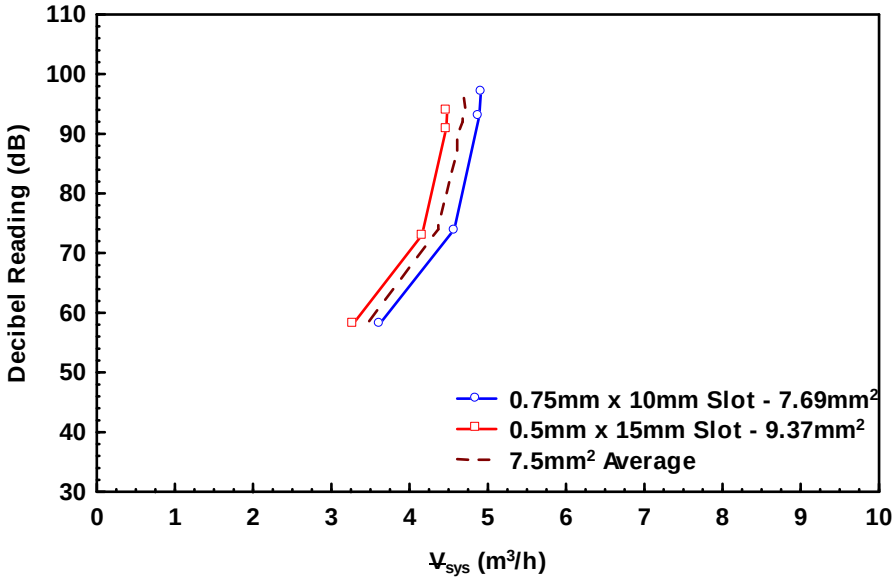

Figure 6.39, Ultrasonic sound level at 0.3m from source plotted against the uncorrected volumetric flow rate for orifices of 7.69mm^2 and 9.37mm^2, at leak pressures of 1.41, 2.01, 4.01, 7.01 Bar$_a$, nominal.

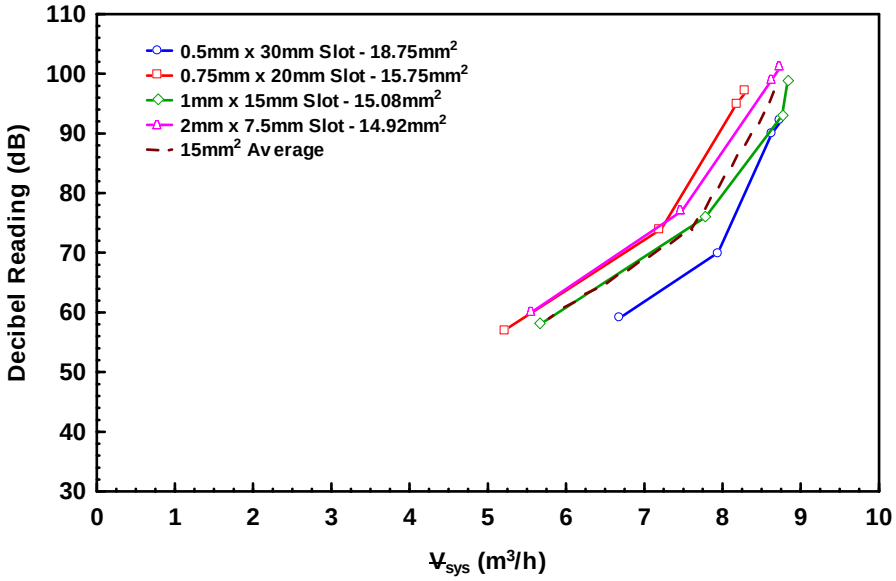

Figure 6.40, Ultrasonic sound level at 0.3m from source plotted against the uncorrected volumetric flow rate for orifices of 18.75mm^2, 15.75mm^2, 15.08mm^2 and 14.92mm^2, at leak pressures of 1.41, 2.01, 4.01, 7.01 Bar$_a$, nominal.

6.6.2 Slot v Round Hole Comparison

In addition to the aspect ratio comparison, two groups were set up to compare slot leaks with round leaks for a common cross sectional area. The measured cross sectional area of the orifices is shown in brackets.

Slot v Round Hole Comparison

1) 2mm^2 1mm x 2mm Slot……..(1.76mm^2)

1.6mm Diameter Hole…….....(2.11mm^2)

2) 8mm^2 1mm x 8mm Slot……..(8.54mm^2)

1.6mm Diameter Hole……..(8.46mm^2)

As with the aspect ratio comparison, Figure 6.41Figure 6.42 show the measured flow through each of the orifices. To allow the effect of the differing geometries of the test pieces to be compared, the volumetric flow rates were corrected for area to take account of the variation in sizes.

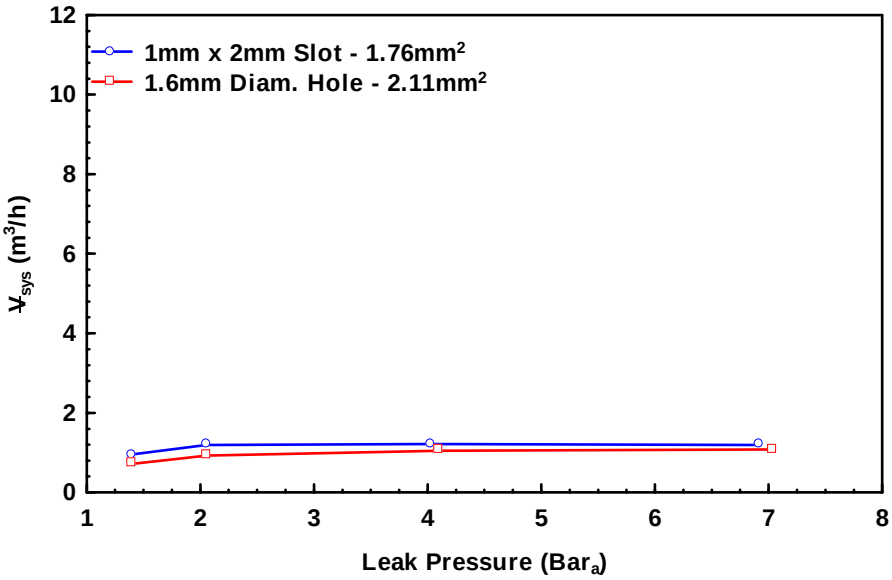

Figure 6.41, Volumetric flow rate comparison of two orifices with cross sectional areas of 1.76mm^2 and 2.11mm^2.

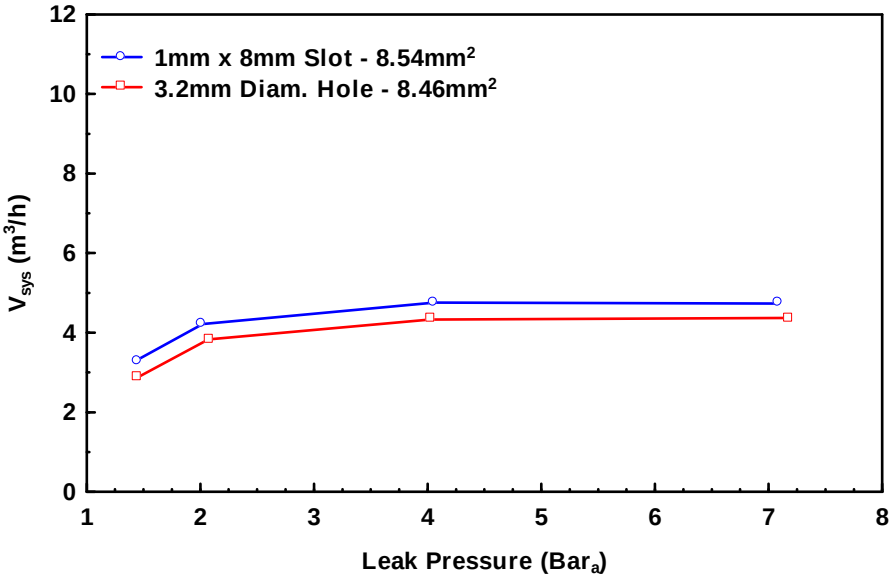

Figure 6.42, Volumetric flow rate comparison of two orifices with cross sectional areas of 8.54mm^2 and 8.46mm^2.

Figure 6.43Figure 6.44, show that, while the small differences in the cross sectional area affected the flow rate of the air through the orifice, they are not significant enough to show any obvious variation between the differing geometries and can be ignored in the development of the leak characterisation chart.

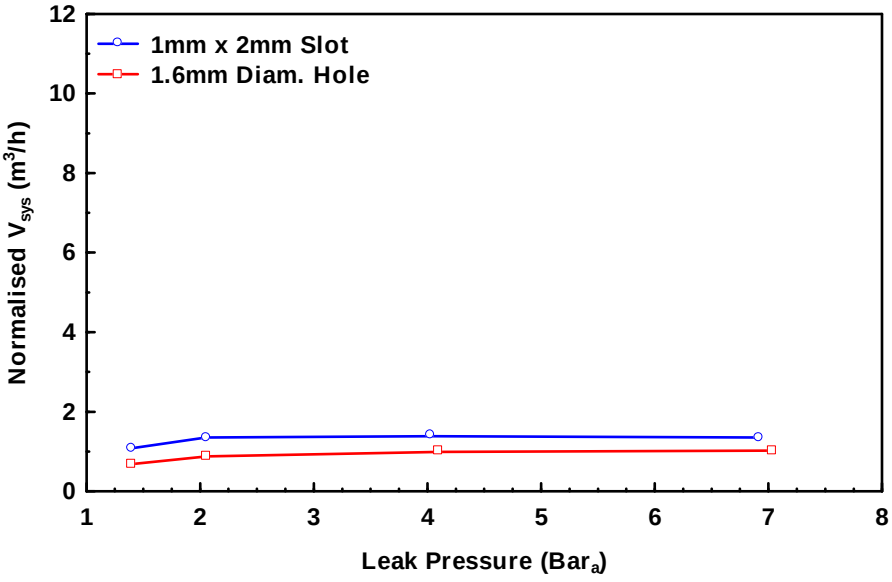

Figure 6.43, Volumetric flow rate normalised to a cross sectional area of 2mm^2.

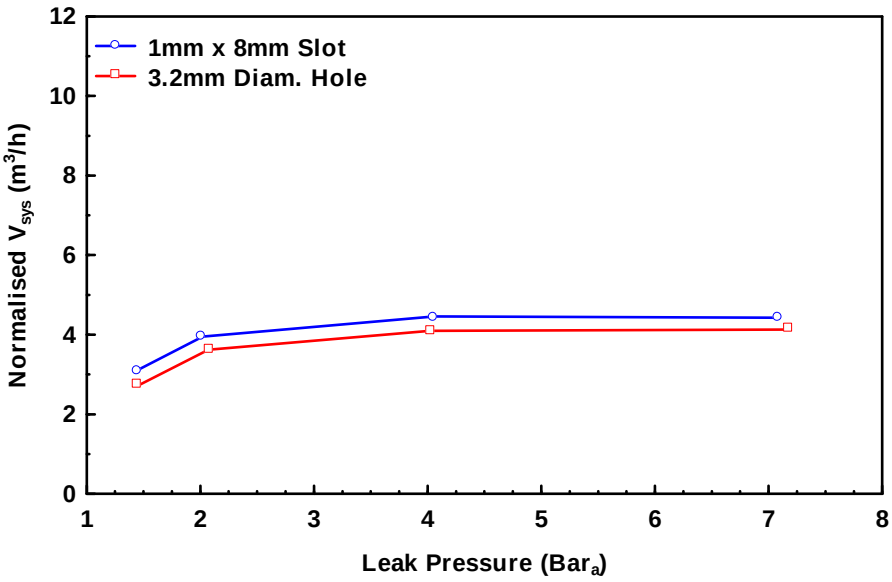

Figure 6.44, Volumetric flow rate normalised to a cross sectional area of 8mm^2.

The ultrasonic sound level in Figure 6.45 shows very little variation between the round hole and the slot, however Figure 6.46 shows an unusually high ultrasonic sound level at 4 Bar_a for the 3.2mm diameter hole. While this is a significant variation, this was the only instance of this elevated ultrasonic sound level through any of the tests, and was attributed to a small burr or inconsistency on the edge of the hole as the flow rate and pressure at that point were within expected limits. As this was an isolated discrepancy it was ignored in the development of the leak characterisation chart.

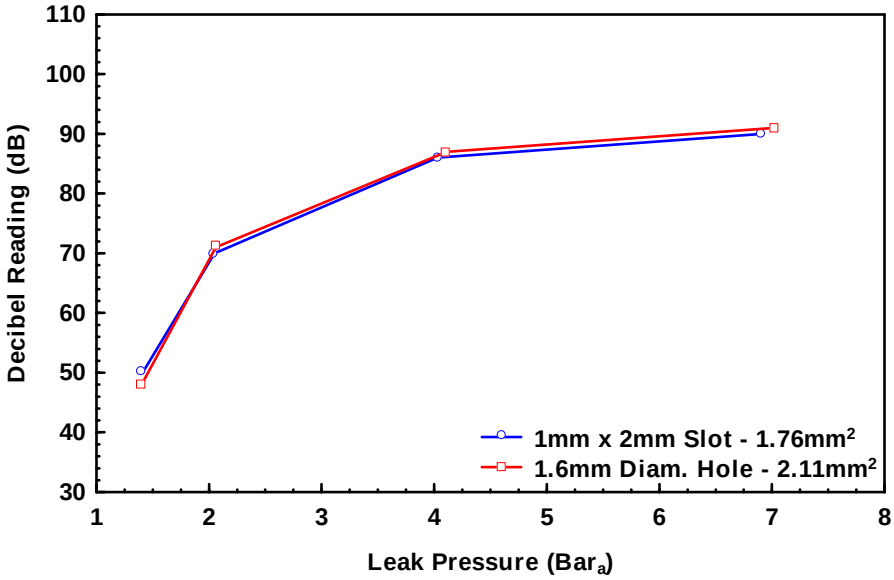

Figure 6.45, Ultrasonic sound level at 0.3m from source for orifices of 1.76mm^2 and 2.11mm^2 at 1.41, 2.01, 4.01, 7.01 Bar$_a$, nominal.

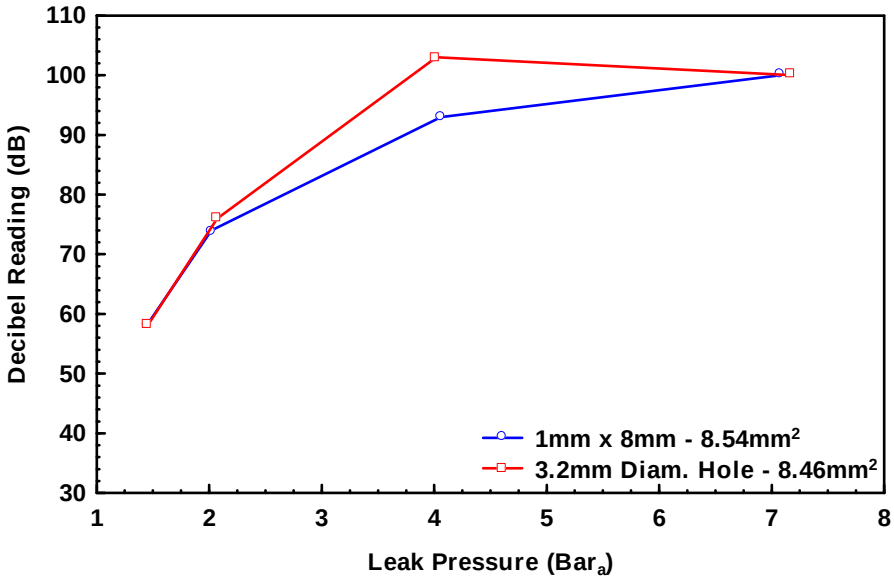

Figure 6.46, Ultrasonic sound level at 0.3m from source for orifices of 8.54mm^2 and 8.46mm^2 at 1.41, 2.01, 4.01, 7.01 Bar$_a$, nominal.

As was noted when comparing the decibel reading against volumetric flow rate in the aspect ratio tests, if an approximate area can be determined for a leak, the volume

flow rate for the actual conditions at the leak can be found for a measured ultrasound level.

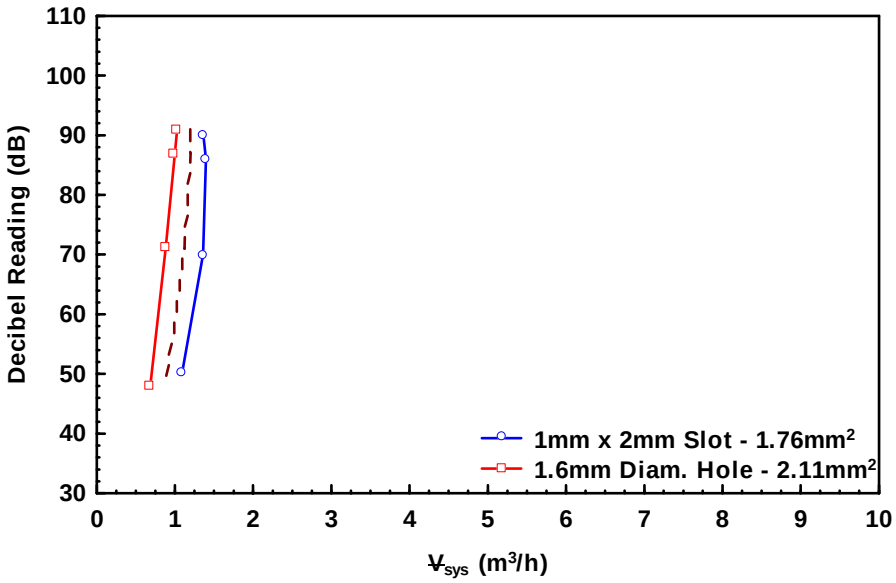

Figure 6.47, Ultrasonic sound level at 0.3m from source plotted against the uncorrected volumetric flow rate for orifices of 1.76mm^2 and 2.11mm^2, at leak pressures of 1.41, 2.01, 4.01, 7.01 Bar$_a$, nominal.

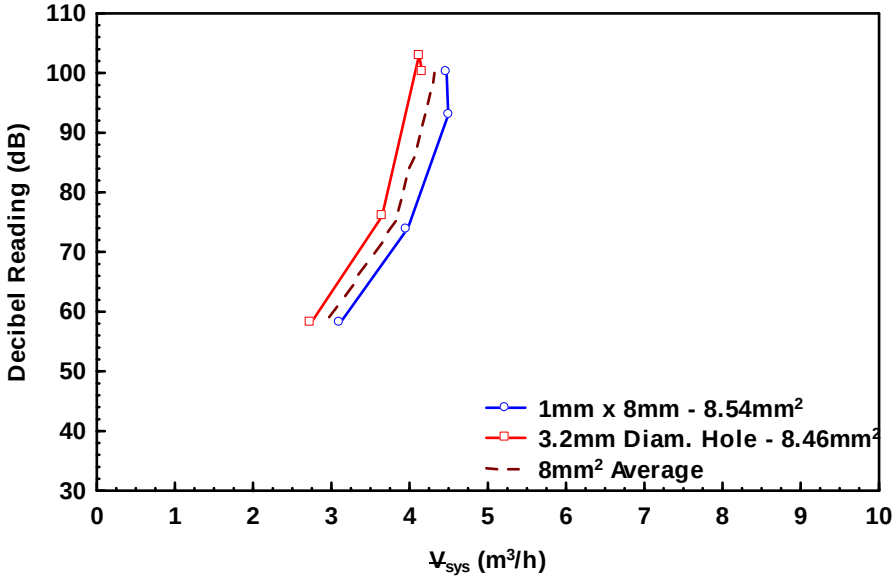

Figure 6.48, Ultrasonic sound level at 0.3m from source plotted against the uncorrected volumetric flow rate for orifices of 8.54mm^2 and 8.46mm^2, at leak pressures of 1.41, 2.01, 4.01, 7.01 Bar$_a$, nominal.

6.6.3 Summary

A number of variations of geometry were tested to determine if leaks of similar sizes but different aspect ratios could be categorised, or alternatively, whether a round hole and a rectangular slot, of the same cross sectional area had differing characteristics. Plotting both volumetric flow rate, and ultrasonic sound level against pressure for each of these scenarios showed no significant variation for any of the alternative geometries. This shows that regular shaped orifices of similar size will give a consistent ultrasound level regardless of variations in shape and do not require any additional correction factor based on leak geometry.

Figure 6.38Figure 6.40 and Figure 6.47Figure 6.48 give a variety of leak sizes for which an approximate loss rate can be obtained for a measured dB reading.

6.7 Coefficient of Discharge

In 6.6 it was stated that the shape of the leak did not have an effect on the flow rate and ultrasound level. While this is true when comparing leak sources with each other, it is not the complete story. When the flow of compressed air through an orifice is calculated using charts for the discharge of air through an orifice, a term C_d is included, this is the coefficient of discharge and for a well rounded hole it is 0.97 while for a sharp edged orifice it is 0.61, both these figures are approximate.

As these figures are very generic and cover a broad spectrum of orifices, more focused values will be calculated to address the individual requirements of a compressed air leak survey.

6.7.1 Calculation of the Coefficient of Discharge

A coefficient of discharge was calculated for each of the leak types to ascertain if this varied between leaks of various types and sizes. When compressed air flows from a

high pressure medium into one of a lower pressure, “an orifice discharge coefficient is used to account for non-ideal effects”, Munson Young & Okiishi (2006).

The following equation is used to calculate the mass flow rate of a fluid through an orifice:

$$\dot{m} = C_d \left(\frac{2}{k+1} \right)^{1/(k-1)} A \frac{P_{Line}}{R T_{Line}} \sqrt{kR \left(\frac{2}{k+1} \right) T_{Line}} \tag{6.1}$$

Rearranging the equation we get:

$$C_d = \frac{\dot{V}}{\left(\frac{2}{k+1} \right)^{1/(k+1)} A \sqrt{kR \left(\frac{2}{k+1} \right) T_{Line}}} \tag{6.2}$$

Where k = 1.4 and R = 0.287 for air.

Each of the following leak types had a coefficient of discharge calculated for it:

1) Tubing of diameters 2.5, 4.0, 6.0mm.
2) Orifice Discs, round holes.
3) Orifice Discs, rectangular slots.

6.7.2 Tubing

Using equation (6.2), the coefficient of discharge was calculated for tubing of diameters 2.5, 4.0 and 6.0mm and lengths 1, 2.5, 5, 7.5, 10 and 25m. A plot of the coefficient of discharge against the leak pressure is shown in Figure 6.49. The critical flow point controls the maximum coefficient of discharge, until this point the flow is not fully developed and the coefficient varies with pressure. Each of the diameters of

tubing, 2.5, 4.0 and 6.0mm have a different coefficient of discharge, these are 0.88, 0.85 and 0.8 respectively for leak pressures above approximately 2.5 Bar_a.

Coefficient of Discharge in Relation to Pressure

While the coefficients of discharge for the three diameters of tubing could be included separately, for the leak characterisation chart the most practical solution is to calculate an average discharge coefficient that can be used in conjunction with any of the three tubing diameters tested. This average ratio was calculated as 0.84.

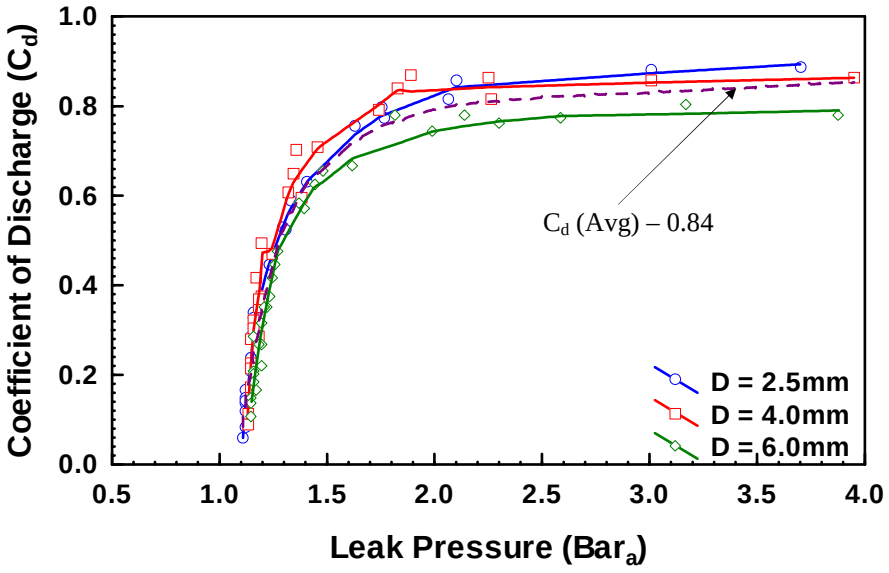

Figure 6.49, Coefficient of discharge calculated for tubing diameters of 2.5, 4.0 and 6.0mm.

6.7.3 Orifice Plates

The coefficient of discharge was calculated for rectangular and round orifices of varying sizes. Plots of the respective coefficients of discharge against the leak pressure are shown in Figure 6.50Figure 6.51. Once again the critical flow point controls the maximum coefficient of discharge.

Coefficient of Discharge in Relation to Pressure

The coefficients of discharge for the rectangular orifice geometries were spread from 0.72 to 0.83 as shown in Figure 6.50 with no apparent trend relating to area or aspect ratio. Part of the variation in the results is as a result of the inaccuracies of the dimensioning of the test pieces as small variations in the cross sectional area of the leak impact significantly on the value of C_d. An average Coefficient of discharge of 0.79 to be used above leak pressures of 4 Bar_a was calculated. To evaluate this, the leak geometries with the maximum and minimum coefficients of discharge, taken at 7 Bar_a, were compared to check how using the average value affected the corrected value of volumetric flow rate. This calculation is shown below.

Using $\dot{V}_{sys}$ for the leak geometries with the max. and min. value of C_d gives:

$\dot{V}_{sys}$(corrected) = $\dot{V}_{sys}$ x C_d(max) = 5.56 x 0.83 = 4.61m^3/h

$\dot{V}_{sys}$(corrected) = $\dot{V}_{sys}$ x C_d(avg) = 5.56 x 0.79 = 4.41m^3/h

This gives a variation in $\dot{V}_{sys}$ of 0.2m^3/h which is a 4% difference.

$\dot{V}_{sys}$(corrected) = $\dot{V}_{sys}$ x C_d(min) = 3.12 x 0.72 = 2.25m^3/h

$\dot{V}_{sys}$(corrected) = $\dot{V}_{sys}$ x C_d(avg) = 3.12 x 0.79 = 2.47m^3/h

This gives a variation in $\dot{V}_{sys}$ of 0.22m^3/h which is a 9% difference.

This result shows that using an average Coefficient of Discharge for the rectangular orifice geometries gives a good level of accuracy and will be included as part of the leak characterisation chart.

The coefficients of discharge for the round orifices showed almost no variation between the different diameters of leak, and an average coefficient of discharge of 0.74 for leak pressures above 4 Bar_a has been included in the leak characterisation chart for round orifices.

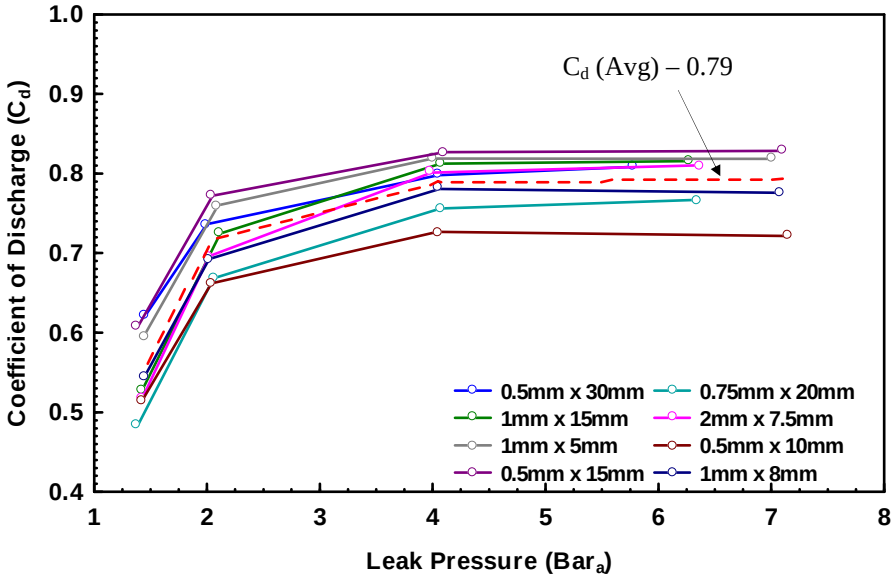

Figure 6.50, Coefficient of discharge calculated for a variety of rectangular shaped orifices.

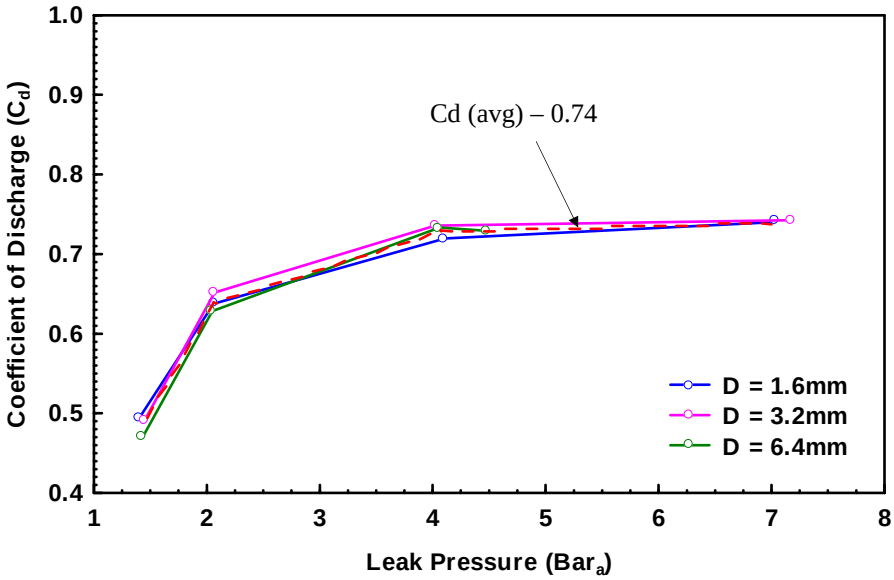

Figure 6.51, Coefficient of discharge calculated for a number of round shaped orifices.

6.7.4 Summary

Compressed air flowing through an orifice requires a coefficient of discharge to account for non ideal effects as the air exits the distribution network. Coefficient profiles have been determined for two of the leak types that can be applied to the

volumetric flow rate for either a known leak pressure. The third, relating to the coefficient of discharge in tubing is affected by the pressure drop through the length of tubing and has therefore been discounted. The length effect shown in 6.5 will be used in its place. The length effect for the tubing and the coefficients of discharge calculated for the orifice plates will allow more accurate estimation of the leak rate by an inspector when conducting a leak survey or audit.

7 Conclusions and Recommendations

7.1 Overview

The use of ultrasonic leak detection to allow industry to quantify air leaks around their plant is fraught with pitfalls. How big is the leak? What type of leak is it? Where in the distribution network is it? The list goes on.

This thesis was written to investigate the main issues facing an inspector when carrying out a leak survey, prioritise them by their impact on the ultrasonic sound level being detected and develop a system for leak characterisation that was more accurate, easy to use in the plant, but could also be more precise if used in conjunction with leak management software that has been developed by the Energy Research Group within the University of Waikato.

Each of the areas of investigation will be addressed in this chapter. A brief introduction covering the current procedures used by UE Systems will be followed by a discussion of the results in each of the areas of research covered in this thesis.

The Research areas are listed below:

1) Directionality of Ultrasound
2) Distance Relationship
3) Length Effect
4) Shape Factor
5) Coefficient of Discharge

This discussion will be followed by a revised leak detection procedure that includes correction factors and graphs that should be used in conjunction with a table of coefficients of discharge through an orifice.

7.2 UE Systems Current Procedure

As was discussed in 3.4, UE Systems supply the “Compressed Air Ultrasonic Leak Detection Guide” which includes a “Guess-timator” chart in conjunction with their Ultraprobe 9000/10000. The guide aids an inspector in estimating the level of air leaks from a compressed air system. It was designed to give an approximation of the total loss rate from the system by measuring the Ultrasonic sound level at a leak and cross referencing it with the supply pressure, this would give an average leak rate for the leak.

One of the main methods recommended for locating a compressed air leak is called the Gross to Fine Method. Starting with the sensitivity dial at maximum, identify the leak, once the leak has been located reduce the sensitivity of the probe. The inspector moves towards the area where the ultrasonic sound level is highest. Using the rubber focusing probe to narrow the detection angle, the ultraprobe is moved from side to side to locate the highest level of ultrasound. As the location of the leak gets closer, the inspector should scan all around the suspected leak area to pinpoint the leak. Then drawing the Ultraprobe back from the leak to a distance of approximately 15” where the Decibel level is measured.

7.3 Research Areas

7.3.1 Directionality of Ultrasound

To ensure greatest accuracy and consistency of results when conducting a leak survey or audit using an ultrasonic leak detector, it is important that the procedure employed maximises the ability of the inspector to obtain consistent results.

The experimental results in this study showed that the peak level of ultrasound is located at approximately 30° to the axis of the flow of air from a leak. The level of ultrasound at wider angles reduces relatively slowly, while the ultrasound on the axis of the flow from a leak is much lower. For situations where the only option is to measure the ultrasound level directly in line with the leak a correction factor of 1.44 can be applied for open ended tubing and 1.33 for an orifice in a line with a leak pressure above 4 Bar_a.

7.3.2 Distance Relationship

During an ultrasonic leak survey it is important that a consistent ultrasonic sound level is obtained. When using the UE Systems ultraprobe, the required distance from the leak is 381mm (15”), as this is the distance that the ultrasound level for different leak rates was measured when building their “Guess-timator” Chart.

This study showed that at 150mm (5.9”) a consistent level of ultrasound was still achieved and this distance will be recommended as the standard measurement in the new leak characterisation chart.

7.3.3 Length Effect

When a leak survey is being conducted there are occasions when compressed air is flowing from an air line with an open end, or from a length of tubing with an orifice in it.

There are two common errors that are made when estimating the leak rate from the air line. The first error is taking the ultrasound reading, but not correcting the supply pressure for the pressure drop effect due to the length of the tubing. The second is the diameter of the tubing, it is important that the inspector is certain that it is the inside diameter of the tubing that is being quoted when estimating the flow rate to ensure the flow rate is not overstated.

It has been shown that for any of the three tubing diameters tested a correction factor of 0.49 can be used for an air leak from a 1m length of tubing leaking air from a distribution network at a pressure of 6 Bar_g.

7.3.4 Shape Factors

The influence of the leak shape on the ultrasound level was investigated to see if there were variations between leaks of different aspect ratios, and other leak geometries, that had constant areas.

The investigation concluded that there were no obvious variations in ultrasound level or volumetric flow rate between different geometries of a constant area.

7.3.5 Coefficient of Discharge

The coefficient of discharge accounts for imperfections in flow at a leak site, these were calculated for a round hole of varying diameter and for a rectangular orifice.

These can be used in conjunction with the leak charts for discharge of air through an orifice shown in Appendix A.

These coefficients of discharge are 0.74 for a round hole and 0.79 for a rectangular orifice.

7.4 Updated Leak Characterisation process

This thesis was concerned with addressing some of the issues that make ultrasonic leak surveys and audits unpredictable. There are two areas of interest, the first addresses the procedural aspects of conducting a leak survey, and the second deals with the application of correction factors and the use of charts to ensure improved accuracy of results.

7.4.1 Procedural changes to leak surveys

Following the results that were found during the course of this thesis there are two main procedural changes that should be made to the current process.

1) When a leak is located and the gross to fine method has been used to isolate the leak, rather than drawing the ultrasonic leak detector directly back from the leak, which will give a very low reading, the loudest signal from the leak source should be identified. If this is not possible, after drawing the leak detector back from the leak in a straight line along the leak axis, a correction factor should be applied to the ultrasound measurement. For a length of tubing with a supply pressure of between 3 – 6 Bar_g this can be taken as 1.44 For leaks directly off a main line when the leak pressure is relatively close to the supply pressure then a correction factor of 1.33 can be used.

Table 7.1, Correction factors for in-line measurement of ultrasound level.

Leak Type	Correction Factor
Tubing (Supply pressure above 3 Bar_g)	1.44
Orifice (Supply pressure above 3 Bar_g)	1.33

2) The measurement of the ultrasound should be taken at 150mm from the leak instead of the current 380mm (15”). As there is no detrimental effect to the consistency of the ultrasound signal having the leak detector at this distance it will be beneficial to be closer top the leak site as it reduces the chance of external factors influencing the measurement.

7.4.2 Volumetric Flow Rate Correction Factors

When estimating the flow rate of the air from a leak, the current process involves taking the ultrasound measurement and supply pressure and looking up the corresponding flow rate. The new process will involve applying correction factors to the leak rates to more accurately represent the leak rate.

These factors are, the length effect correction factor for open ended tubing and coefficient of discharge correction factors for round holes and rectangular orifices.

The length effect factor varies with supply pressure, but for a 6 Bar_g supply pressure can be taken as 0.5 at 1m or 0.22 at 5m.This is shown in the abbreviated Table 7.2. The full table of correction factors can be found in table 6.4.

Table 7.2, Correction factors for length effect

Length effect (D = 2.5, 4.0, 6.0mm)	Correction Factor
1m (Supply pressure 6 Bar_g)	0.5
5m (Supply pressure 6 Bar_g)	0.22

The coefficient of discharge correction factors for supply pressures above 3 Bar_g are 0.74 for a round hole and 0.79 for a rectangular slot. This is shown in Table 7.3.

Table 7.3, Correction factors for coefficient of discharge.

Coefficient of Discharge	Correction Factor
Round Holes (Leak pressure above 3 Bar_g)	0.74
Rectangular Slots (Leak pressure above 3 Bar_g)	0.79

7.4.3 Recommendations for Future Study

1) Conduct experiments on the effect on the ultrasonic sound level of various flange leaks and thread leaks.

2) Further investigation on the length effect to examine at what diameter of hole in the line the flow through the leak becomes the dominant path for the air in the distribution network.

3) Additional experimental work at higher supply pressures, (up to 10 Bar_g).

8 References

ASTM International. (2005). E 1002 – 05. Standard Testing Method for Leaks using Ultrasonics.

Bies, David A., Hanson, Colin H. (1998). Engineering Noise Control - Theory and Practice, 2nd Edition. E & FN Spon.

Cengal, Yunus A. & Boles, Michael A. (2006). Thermodynamics – an engineering approach, fifth edition. McGraw Hill Higher Education.

Compressed Air Sourcebook. U.S. Department of Energy Lawrence Berkeley National Laboratory. Washington DC and Resource Dynamics Corporation. Vienna, VA

Davidson P. A. (2004). Turbulence – An introduction for scientists and engineers. Oxford.

Ecompressedair – http://www.compressedair.com/library/compressedair history.shtml

\Everest, F. Alton. (1994). Master Handbook of Engineering Acoustics, 3rd Edition, McGraw Hill.

Fahy, Frank. (2001). Foundations of Engineering acoustics, Elselvier Academic Press.

Munson, Bruce R., Young, Donald F. & Okiishi, Theodore H. (2006). Fundamentals of Fluid Mechanics. Wiley

Pope, Stephen B. (2000). Turbulent Flows. Cambridge University Press.

UE Systems, (1997). Airborne Ultrasound Level 1 Handbook. First Edition.

White, Frank M., (1994). Fluid Mechanics, Third Edition. McGraw Hill.

9 Appendices

9.1 Appendix A

Discharge of Air Through an Orifice (Imperial)

Gauge Pressure before Orifice in Pounds per sq. in.	Diameter of Orifice										
	1/64"	1/32"	1/16"	1/8"	1/4"	3/8"	1/2"	5/8"	3/4"	7/8"	1"
	Discharge in cubic feet of free air per minute										
1	0.028	0.112	0.45	1.8	7.18	16.2	28.7	45	64.7	88.1	115
2	0.04	0.158	0.633	2.53	10.1	22.8	40.5	63.3	91.2	124	162
3	0.048	0.194	0.775	3.1	12.4	27.8	49.5	77.5	111	152	198
4	0.056	0.223	0.892	3.56	14.3	32.1	57	89.2	128	175	228
5	0.062	0.248	0.993	3.97	15.9	35.7	63.5	99.3	143	195	254
6	0.068	0.272	1.09	4.34	17.4	39.1	69.5	109	156	213	278
7	0.073	0.293	1.17	4.68	18.7	42.2	75	117	168	230	300
9	0.083	0.331	1.32	5.3	21.20	47.7	84.7	132	191	260	339
12	0.095	0.379	1.52	6.07	24.3	54.6	97	152	218	297	388
15	0.105	0.42	1.68	6.72	26.9	60.5	108	168	242	329	430
20	0.123	0.491	1.96	7.86	31.4	70.7	126	196	283	385	503
25	0.14	0.562	2.25	8.98	35.9	80.9	144	225	323	440	575
30	0.158	0.633	2.53	10.1	40.5	91.1	162	253	365	496	648
35	0.176	0.703	2.81	11.3	45	101	180	281	405	551	720
40	0.194	0.774	3.1	12.4	49.6	112	198	310	446	607	793
45	0.211	0.845	3.38	13.5	54.1	122	216	338	487	662	865
50	0.229	0.916	3.66	14.7	58.6	132	235	366	528	718	938
60	0.264	1.06	4.23	16.9	67.6	152	271	423	609	828	1082
70	0.3	1.2	4.79	19.2	76.7	173	307	479	690	939	1227
80	0.335	1.34	5.36	21.4	85.7	193	343	536	771	1050	1371
90	0.37	1.48	5.92	23.7	94.8	213	379	592	853	1161	1516
100	0.406	1.62	6.49	26	104	234	415	649	934	1272	1661
110	0.441	1.76	7.05	28.2	113	254	452	705	1016	1383	1806
120	0.476	1.91	7.62	30.5	122	274	488	762	1097	1494	1951
125	0.494	1.98	7.9	31.6	126	284	506	790	1138	1549	2023
150	0.582	2.37	9.45	37.5	150	338	600	910	1315	1789	2338
200	0.761	3.1	12.35	49	196	441	784	1225	1764	2401	3136
250	0.935	3.8	15.18	60.3	241	542	964	1508	2169	2952	3856
300	0.995	4.88	18.08	71.8	287	646	1148	1795	2583	3515	4592
400	1.22	5.98	23.81	94.5	378	851	1512	2360	3402	4630	6048
500	1.519	7.14	29.55	117.3	469	1055	1876	2930	4221	5745	7504
750	2.24	10.98	43.85	174	696	1566	2784	4350	6264	8525	11136
1000	2.985	14.6	58.21	231	924	2079	3696	5790	8316	11318	14784

This table is based on 100% coefficient of flow.

9.2 Appendix B

Discharge of Air Through an Orifice (Metric)

Gauge Pressure before Orifice in Bar	Diameter of Orifice (mm)										
	0.5	1	2	3	4	5	7	10	15	20	25
	Discharge of air in cubic metres per hour at 1 bar abs. and 15 degrees C										
0.5	0.1944	0.7812	3.1284	7.0416	12.517	19.559	38.34	78.228	176.04	312.59	488.88
1	0.2736	1.0908	4.3668	9.8244	17.464	27.284	53.496	109.15	245.56	436.68	682.2
2	0.4104	1.638	6.5484	14.735	27.814	40.932	80.208	163.73	368.28	654.84	1023.1
3	0.5472	2.1816	8.73	19.645	34.927	54.576	106.96	218.3	491.04	873	1364.4
4	0.6804	2.7288	10.915	24.556	43.668	68.22	133.7	272.84	613.8	1091.5	1711.8
5	0.8172	3.276	13.097	29.47	52.38	81.828	160.45	326.12	736.56	1309.7	2046.6
6	0.954	3.8196	15.278	34.38	71.928	95.508	187.16	381.96	859.68	1527.8	2387.5
7	1.0908	4.3668	17.464	39.276	73.44	109.15	213.91	436.68	982.44	1746.4	2728.4
8	1.2276	4.9104	19.645	44.208	78.588	122.8	240.66	491.04	1105.2	1964.5	3069.7
9	1.3644	5.4576	21.827	49.104	87.3	136.44	267.41	545.76	1228	2182.7	3410.6
10	1.5012	6.0012	24.012	54.036	96.048	150.08	294.16	600.12	1350.7	2401.2	3751.2
12	1.7748	7.0956	28.375	63.864	113.51	177.37	347.62	709.56	1596.2	2837.5	4435.2
15	2.1816	8.7336	34.927	78.588	139.72	218.3	427.68	873.36	1964.5	3492.7	5457.6
20	2.8656	11.459	45.828	103.14	183.35	286.49	561.6	1145.9	2578.7	4582.8	7164

This Table is based on 100% coefficient of flow.